Multiple double-pole bright-bright and bright-dark solitons and energy-exchanging collision in the M-component nonlinear Schrödinger equations

Jiguang Rao,[1,2,3] T. Kanna,[4] K. Sakkaravarthi,[4,5] and Jingsong He[1,*]

[1]*Institute for Advanced Study, Shenzhen University, Shenzhen, Guangdong 518060, People's Republic of China*

[2]*Institute of Microscale Optoelectronics, Shenzhen University, Shenzhen, Guangdong 518060, People's Republic of China*

[3]*School of Mathematics and Statistics, Hubei University of Science and Technology, Xianning, Hubei 437100, People's Republic of China*

[4]*Nonlinear Waves Research Lab, PG and Research Department of Physics, Bishop Heber College (Autonomous), Affiliated to Bharathidasan University, Tiruchirappalli 620 017, Tamil Nadu, India*

[5]*Centre for Nonlinear Dynamics, School of Physics, Bharathidasan University, Tiruchirappalli 620 024, India*

(Received 20 October 2020; accepted 1 June 2021; published 25 June 2021)

Multiple double-pole bright-bright and bright-dark soliton solutions for the multicomponent nonlinear Schrödinger (MCNLS) system comprising three types of nonlinearities, namely, focusing, defocusing, and mixed (focusing-defocusing) nonlinearities, arising in different physical settings are constructed. An interesting type of energy-exchanging phenomenon during collision of these double-pole solitons is unraveled. To explore the objectives, we consider the general solutions of a set of generalized MCNLS equations and by taking the long-wavelength limit with proper parameter choices of single-pole bright-bright and bright-dark soliton pairs, the multiple double-pole bright-bright and bright-dark soliton solutions are constructed in terms of determinants. The regular double-pole bright-bright solitons exist in the focusing and focusing-defocusing MCNLS equations and undergo a particular type of energy-sharing collision for $M \geqslant 2$ in addition to the usual elastic collisions. A striking feature observed in the process of energy-sharing collisions is that the double-pole two-soliton possessing unequal intensities before collision indeed exactly exchange their intensities after collision. Further, the existence of double-pole bright-dark solitons in the MCNLS equations with focusing, defocusing, and mixed (focusing-defocusing) nonlinearities is analyzed by constructing explicit determinant form solutions, where the double-pole bright solitons exhibit elastic and energy-exchanging collisions while the double-pole dark solitons undergo mere elastic collision. The double-pole bright-dark solitons possess much richer localized coherent patterns than their counterpart double-pole bright-bright solitons. For particular choices of parameters, we demonstrate that the solitons would degenerate into the background, resulting in a lower number of solitons. Another important observation is the formation of doubly localized rogue waves with extreme amplitude, in the case of double-pole bright-dark four-solitons. Our results should stimulate interest in such special multipole localized structures and are expected to have ramifications in nonlinear optics.

DOI: 10.1103/PhysRevE.103.062214

I. INTRODUCTION

Over the past two decades or so, the study of the family of multiple coupled (vector) nonlinear evolution equations (NLEEs) has attracted considerable research interest [1–4]. In general, these systems have been studied extensively in nonlinear optics [1] and in the setting of Bose-Einstein condensates [5]. In optics, such multicomponent systems arise in the description of propagation of orthogonally polarized pulses in birefringent media [6], fiber Bragg grating [7], metamaterials [8], parametric three-wave interaction processes [9], incoherent beam propagation in nonlinear waveguides [10], etc. In contrast, the dynamics of multiple-species atomic condensates or mixtures of spin states of a given atomic species can be very well described in the framework of such a type of multicomponent NLEE in the mean-field approximation [5]. Generally, these systems are nonintegrable and become integrable for particular sets of system parameters [2,11], which are experimentally feasible. One such versatile family of NLEEs is the nonlinear Schrödinger-type equations. These systems feature several intriguing nonlinear coherent structures that display several interesting dynamical behaviors. For example, the bright solitons in the Manakov system [12], a prototypical system for the multicomponent nonlinear Schrödinger (MCNLS) family of equations, undergo fascinating shape-changing collisions [13]; the partially coherent solitons in such MCNLS equations exhibit variable shape [14,15]; the symbiotic (bright-dark) solitons in the 2CNLS system can display boomeronic behavior (coherent structures that reverse their dynamics spontaneously) [16]; and multicomponent rogue waves with exotic profiles appear [17,18]. In higher dimensions the variants of such multicomponent CNLS systems display still more novel phenomena such as spatiotemporal multimode optical solitons [19], fission of solitons into a lump coherent structure and fusion of a lump into solitons [20], expanding necklace ring solitons [21], and resonant solitons with intricate structures [22]

*Corresponding author: hejingsong@szu.edu.cn

(for a detailed review one may refer to [23] and references therein).

In this work we consider the versatile integrable MCNLS system

$$iu_{\ell,z} + u_{\ell,tt} + 2u_\ell \sum_{k=1}^{M} \delta_k |u_k|^2 = 0, \quad \ell = 1, 2, \ldots, M, \quad (1)$$

where u_ℓ, $\ell = 1, 2, \ldots, M$, denotes the complex amplitude of the ℓth component, z and t denote the normalized evolution and spatial coordinates, respectively, and the nonlinearity coefficients δ_ℓ are real parameters. As mentioned before, the above set of MCNLS equations is of much physical significance. For example, similar multicomponent nonlinear Schrödinger equations appear in describing the dynamics of wavelength division multiplexing high-bit-rate communication systems [24], multichannel bit-parallel wavelength optical fiber networks [25], ultrashort-pulse propagation in multimode fibers [26], and the setting of propagation of mutually incoherent wave packets in Kerr-like photorefractive media [10]. It can be noticed that for $M = 2$ with all δ_ℓ being equal and positive, the above system (1) reduces to the celebrated Manakov system [12]. The Manakov system supports bright solitons that display a kind of fascinating energy-sharing collision behavior [13], where there is an energy redistribution among the colliding bright solitons that takes place with the preservation of total intensity, thereby changing the amplitude of the solitons before and after collision. This type of collision was experimentally demonstrated in Ref. [27]. The 2CNLS system features bright-dark [28–30] and dark-dark solitons [28] for other sign combinations of δ_ℓ. Interestingly, the 2CNLS system with mixed signs of (focusing-defocusing) nonlinearity supports bright solitons that exhibit a special type of energy-exchanging collision scenario that is different from that of the Manakov system [31]. The Manakov system also hosts rogue waves with different special structures [16,18,32].

It should be noted that not only the 2CNLS system, but also the 3CNLS as well as MCNLS systems with $M > 3$ are of considerable importance. Indeed, the MCNLS system possesses rich dynamical features and shows several distinct possibilities of energy-sharing collision of bright solitons [33–35] and bright-dark solitons [30] depending upon the nature of the nonlinearities (whether they are focusing or defocusing or mixed type). Thus, following the Manakov system, an extensive studies of multiple coupled nonlinear Schrödinger systems have been carried out and the bright [36,37], dark [38,39], and bright-dark solitons [40,41] of the MCNLS system have been reported.

This paper is devoted to the study of coherent structures, specifically double-pole solitons in the MCNLS system (1). In fact, the higher-order pole solitons have been known since the seminal work of Zakharov and Shabat [42] on the standard focusing nonlinear Schrödinger equation [i.e., $M = 1$ with $\delta_1 > 0$ in Eq. (1)], where soliton solutions with spectral data consisting of higher-order poles were reported. It is important to note the nature of multisoliton collisions in several physically interesting nonlinear integrable systems undergone in a pairwise manner, where the phases of each interacting soliton make them collide at different points during propagation. Such pairwise soliton collisions exhibiting systems include the celebrated Korteweg–de Vries model, sine-Gordon equations, nonlinear Schrödinger (NLS) equations, the Manakov system, the MCNLS system, M-component Gross-Pitaevskii equations, M-component Yajima-Oikawa equations, the higher-dimensional M-component long-wave–short-wave resonance interaction model, etc., arising in different contexts like shallow water waves, nonlinear optics, Bose-Einstein condensates, hydrodynamics, ion-acoustic waves, and plasma systems. However, such pairwise interaction can be controlled by incorporating an additional parameter in the exact solutions, which tunes the phases of the associated solitons and introduces multiparticle effects. This idea of manipulating the phases of interacting solitons to tailor the collision point was coined in the literature and referred to as the coalescence of wave numbers and multiple-pole solitons [43–71]. To be precise, the higher-order pole bright solitons of the standard focusing NLS equation have been investigated from different perspectives so far, for example, multipole N-soliton interaction [43], algebraic aspects of multipole solitons [44–46], long-time asymptotic behavior for the fixed pole-order solitons [47,48], and large-order asymptotics for multiple-pole solitons [49]. The solitons admitting higher-order poles have also been studied for the modified Korteweg–de Vries equation [50,51], the sine-Gordon equation [52–54], the N-wave system [55], the coupled Sasa-Satsuma system [56], the Hirota equation [57–59], and several other nonlinear evolution equations [60–69].

Although there exist a number of works on the high-order pole solitons for the standard focusing NLS equation, results are scarce for the study of such solitons with higher-order poles and their subsequent collision dynamics in the MCNLS equations (1). There exist numerous interesting phenomena which one has to pay attention to in order to realize the full potentialities of the multicomponent higher-order pole solitons in the system (1). A double-pole two bright two-soliton solution has been presented for the focusing 2CNLS equations [i.e., $M = 2$ and $\delta_1 = \delta_2 = 1$ in Eq. (1)] in the original study of Chow and Lai [70], which itself requires further analysis in view of the intricate dynamical properties of multicomponent solitons [34,35]. Specifically, in the literature, only the elastic collision process of double-pole solitons has been addressed; the energy-sharing collisions of double-pole solitons were not observed, which is quite possible in multicomponent solitons. For the double-pole bright-dark solitons, Biondini and Kraus [71] considered double zeros of the analytic scattering coefficients in the inverse scattering transform technique and presented a double-pole bright-dark soliton solution for the defocusing Manakov system [i.e., $M = 2$ and $\delta_1 = \delta_2 = -1$ in Eq. (1)], but the collision behavior of the double-pole bright-dark solitons was not studied in their work. Apart from the study of collision dynamics, it is quite natural to raise the question of the possibility of different types of shape-changing (energy-sharing) collisions of such double-pole solitons. Another interesting aspect that needs attention is to look for the appearance of composite double-pole bright-dark solitons and to explore their collisional features as well as their role in the formation of the most recently much studied objects, namely, Peregrine solitons and rogue waves.

Thus, the objective of this paper is threefold. First is to construct a double-pole N-soliton solution comprising M bright components of the integrable MCNLS system (1) and second is to obtain double-pole N-solitons admitting $M-1$ bright components along with a dark component. Our third aim is to perform a detailed analysis of their dynamical features, which includes the interesting energy-sharing collisions of these bright-bright and bright-dark double-pole solitons.

This paper is organized as follows in order to address the above-mentioned studies. In Sec. II we first construct the multiple double-pole bright solitons for the MCNLS equations (1) in the form of determinants by taking the long-wavelength limit of bright solitons in a pairwise manner with proper parameter choices. Then we study the double-pole M bright two-soliton collision scenario and investigate energy (intensity)-exchanging collision dynamics in detail in addition to the double-pole M bright four-soliton collisions. In Sec. III we present the multiple double-pole bright-dark soliton solutions, comprising bright solitons in $M-1$ components and dark solitons in a single component, for the MCNLS equation and study the dynamics of the bright-dark soliton collisions as well as the formation of rogue waves. A brief summary of the obtained results and certain possible future directions of study are given in Sec. IV.

II. MULTIPLE DOUBLE-POLE M BRIGHT $2N$-SOLITONS OF THE MCNLS EQUATIONS AND ENERGY-EXCHANGING COLLISION

In this section we obtain the N double-pole solitons spread among M bright components (hereafter referred to as double-pole M bright N-solitons). The idea behind the construction of these multicomponent double-pole bright solitons from the general $2N$ bright soliton solutions of the MCNLS equations (1) is to select N pairs of wave numbers in which each pair consists of wave numbers with equal magnitude but of opposite signs. Then, considering a special limit, such that their imaginary parts are very small, and with an appropriate choice of phase factors, one can arrive at the desired double-pole M bright N-soliton solution. This is done by choosing the parameters in Eq. (A2) as

$$\begin{aligned} K &= 2N, \\ p_{N+s} &= -p_s, \\ e^{\xi_{j,0}} &= \tilde{\xi}_{j,0} p_{jI} e^{(\pi/2)i}, \\ e^{\eta^{(\ell)}_{j,0}} &= \tilde{\eta}^{(\ell)}_{j,0} p_{jI} e^{(\pi/2)i}, \end{aligned} \tag{2}$$

$$\tilde{\xi}_{s,0}\tilde{\xi}_{N+s,0} + \sum_{k=1}^{M} \delta_k \tilde{\eta}^{(k)}_{s,0}\tilde{\eta}^{(k)}_{N+s,0} = 0$$

and by taking the limit $p_{sI} \to 0$ for $s = 1, 2, \ldots, N$. Here and in the following R and I appearing in the subscript represent the real and imaginary parts of a given parameter or function, respectively.

The resulting set of double-pole M bright N-soliton solutions of the MCNLS equations (1) can be cast as

$$u_\ell = \frac{g^{(\ell)}(t,z)}{f(t,z)}, \quad \ell = 1, 2, \ldots, M, \tag{3}$$

where

$$\begin{aligned} f &= \begin{vmatrix} \tilde{m}_{s,j} & \tilde{m}_{s,N+j} \\ \tilde{m}_{N+s,j} & \tilde{m}_{N+s,N+j} \end{vmatrix}_{1\leqslant s,j\leqslant N}, \\ g^{(\ell)} &= \begin{vmatrix} \tilde{m}_{s,j} & \tilde{m}_{s,N+j} & \tilde{\phi}_s \\ \tilde{m}_{N+s,N+j} & \tilde{m}_{N+s,N+j} & \tilde{\phi}_{N+s} \\ i\tilde{\eta}^{(\ell)}_{j,0} & i\tilde{\eta}^{(\ell)}_{N+j,0} & 0 \end{vmatrix}_{1\leqslant s,j\leqslant N}. \end{aligned} \tag{4}$$

The matrix elements appearing in Eqs. (4) are given by

$$\tilde{m}_{s,j} = \frac{\tilde{\xi}_{s,0}\tilde{\xi}_{j,0} e^{(p_{sR}+p_{jR})t + i(p_{sR}^2 - p_{jR}^2)z}}{p_{sR}+p_{jR}} + \frac{\sum_{k=1}^{M} \delta_k \tilde{\eta}^{(k)}_{s,0}\tilde{\eta}^{(k)}_{j,0}}{p_{sR}+p_{jR}},$$

$$\tilde{m}_{N+s,N+j} = -\frac{\tilde{\xi}_{N+s,0}\tilde{\xi}_{N+j,0} e^{-(p_{sR}+p_{jR})t + i(p_{sR}^2 - p_{jR}^2)z}}{p_{sR}+p_{jR}} - \frac{\sum_{k=1}^{M} \delta_k \tilde{\eta}^{(k)}_{N+s,0}\tilde{\eta}^{(k)}_{N+j,0}}{p_{sR}+p_{jR}},$$

and, for $s \neq j$,

$$\tilde{m}_{s,N+j} = \frac{\tilde{\xi}_{s,0}\tilde{\xi}_{N+j,0} e^{(p_{sR}-p_{jR})t + i(p_{sR}^2 - p_{jR}^2)z}}{p_{sR}-p_{jR}} + \frac{\sum_{k=1}^{M} \delta_k \tilde{\eta}^{(k)}_{s,0}\tilde{\eta}^{(k)}_{N+j,0}}{p_{sR}-p_{jR}},$$

$$\tilde{m}_{N+s,j} = \frac{\tilde{\xi}_{N+s,0}\tilde{\xi}_{j,0} e^{(-p_{sR}+p_{jR})t + i(p_{sR}^2 - p_{jR}^2)z}}{-p_{sR}+p_{jR}} + \frac{\sum_{k=1}^{M} \delta_k \tilde{\eta}^{(k)}_{N+s,0}\tilde{\eta}^{(k)}_{j,0}}{-p_{sR}+p_{jR}}$$

and

$$\begin{aligned} \tilde{m}_{s,N+s} &= \tilde{\xi}_{s,0}\tilde{\xi}_{N+s,0}(t + 2ip_{sR}z), \\ \tilde{m}_{N+j,j} &= \tilde{\xi}_{N+j,0}\tilde{\xi}_{j,0}(t - 2ip_{jR}z), \end{aligned}$$

along with

$$\begin{aligned} \tilde{\phi}_s &= i\tilde{\xi}_{s,0} e^{p_{sR}t + ip_{sR}^2 z}, \\ \tilde{\phi}_{N+s} &= i\tilde{\xi}_{N+s,0} e^{-p_{sR}t + ip_{sR}^2 z}. \end{aligned}$$

Here p_{sR}, $\tilde{\xi}_{s,0}$, $\tilde{\eta}^{(\ell)}_{j,0}$, $\tilde{\xi}_{N+s,0}$, and $\tilde{\eta}^{(\ell)}_{N+j,0}$ $(\ell = 1, 2, \ldots, M)$ are real parameters and the parameters $\tilde{\xi}_{s,0}$, $\tilde{\eta}^{(\ell)}_{j,0}$, $\tilde{\xi}_{N+s,0}$, and $\tilde{\eta}^{(\ell)}_{N+j,0}$ are subject to the following parametric condition:

$$\tilde{\xi}_{s,0}\tilde{\xi}_{N+s,0} + \sum_{k=1}^{M} \delta_k \tilde{\eta}^{(k)}_{s,0}\tilde{\eta}^{(k)}_{N+s,0} = 0. \tag{5}$$

In order to explore the salient features of double-pole solitons, in the following section we deduce explicit forms of double-pole two- and four-soliton solutions from the above general N-soliton solution and investigate their propagation as well as collision dynamics in detail with categorical analysis and graphical demonstrations.

A. Double-pole M bright two-solitons and energy-exchanging collision

We start with the simplest double-pole M bright two-soliton solution and their collision dynamics in the MCNLS

equations (1). By taking $N = 1$ in the general solution (4), the double-pole M bright two-soliton solution (3) of the MCNLS equations (1) can be derived and the determinant forms of the functions f and $g^{(\ell)}$ can be explicitly written as

$$f = \begin{vmatrix} \tilde{m}_{1,1} & \tilde{m}_{1,2} \\ \tilde{m}_{2,1} & \tilde{m}_{2,2} \end{vmatrix}, \quad g^{(\ell)} = \begin{vmatrix} \tilde{m}_{1,1} & \tilde{m}_{1,2} & \phi_1 \\ \tilde{m}_{2,1} & \tilde{m}_{2,2} & \phi_2 \\ i\tilde{\eta}_{1,0}^{(\ell)} & i\tilde{\eta}_{2,0}^{(\ell)} & 0 \end{vmatrix}, \tag{6}$$

where $\tilde{m}_{1,1} = \frac{1}{2p_{1R}}(\tilde{\xi}_{1,0}^2 e^{2p_{1R}t} + \sum_{k=1}^{M} \delta_k \tilde{\eta}_{1,0}^{(k)2})$, $\tilde{m}_{1,2} = \tilde{\xi}_{1,0}\tilde{\xi}_{2,0}(t + 2ip_{1R}z)$, $\tilde{m}_{2,1} = \tilde{\xi}_{1,0}\tilde{\xi}_{2,0}(t - 2ip_{1R}z)$, $\tilde{m}_{2,2} = -\frac{1}{2p_{1R}}(\tilde{\xi}_{2,0}^2 e^{-2p_{1R}t} + \sum_{k=1}^{M} \delta_k \tilde{\eta}_{2,0}^{(k)2})$, $\phi_1 = i\tilde{\xi}_{1,0}e^{p_{1R}t+ip_{1R}^2 z}$, $\phi_2 = i\tilde{\xi}_{2,0}e^{-p_{1R}t+ip_{1R}^2 z}$, and the real parameters $\tilde{\xi}_{j,0}$, $\tilde{\eta}_{j,0}^{(\ell)}$ $(j = 1, 2)$ fulfill the parametric constraint defined in (5), namely, $\tilde{\xi}_{1,0}\tilde{\xi}_{2,0} + \sum_{k=1}^{M} \delta_k \tilde{\eta}_{1,0}^{(k)}\tilde{\eta}_{2,0}^{(k)} = 0$. Further, the above double-pole M bright two-soliton solution can be rewritten in terms of the algebraic-hyperbolic form

$$\begin{aligned} f = & -\frac{1}{2p_{1R}^2}\left(\sum_{k=1}^{M} \delta_k \tilde{\eta}_{1,0}^{(k)}\tilde{\eta}_{2,0}^{(k)}\tilde{\xi}_{1,0}\tilde{\xi}_{2,0}\right)\cosh\left(2p_{1R}t + \tilde{\tilde{\eta}}_{2,0}^{(k)} - \tilde{\tilde{\eta}}_{1,0}^{(k)} + \tilde{\tilde{\xi}}_{1,0} - \tilde{\tilde{\xi}}_{2,0}\right) \\ & - \frac{1}{4p_{1R}^2}\left(\sum_{k=1}^{M} \delta_k \tilde{\eta}_{1,0}^{(k)2}\right)\left(\sum_{k=1}^{M} \delta_k \tilde{\eta}_{2,0}^{(k)2}\right) - \tilde{\xi}_{1,0}^2\tilde{\xi}_{2,0}^2(t^2 + 4p_{1R}^2 z^2), \\ g^{(\ell)} = & \sqrt{\tilde{\eta}_{1,0}^{(\ell)}\tilde{\eta}_{2,0}^{(\ell)}\tilde{\xi}_{1,0}\tilde{\xi}_{2,0}}\frac{e^{ip_{1R}^2 z}}{p_{1R}^2}\Bigg[2\tilde{\xi}_{1,0}\tilde{\xi}_{2,0}p_{1R}t\cosh\left(p_{1R}t + \tfrac{1}{2}\left(\tilde{\tilde{\eta}}_{2,0}^{(\ell)} - \tilde{\tilde{\eta}}_{1,0}^{(\ell)} + \tilde{\tilde{\xi}}_{1,0} - \tilde{\tilde{\xi}}_{2,0}\right)\right) \\ & + \left(1 + 4ip_{1R}^2 z\right)\tilde{\xi}_{1,0}\tilde{\xi}_{2,0}\sinh\left(p_{1R}t + \tfrac{1}{2}\left(\tilde{\tilde{\eta}}_{2,0}^{(\ell)} - \tilde{\tilde{\eta}}_{1,0}^{(\ell)} + \tilde{\tilde{\xi}}_{1,0} - \tilde{\tilde{\xi}}_{2,0}\right)\right) \\ & - \sum_{k=1}^{M} \delta_k \sqrt{\tilde{\eta}_{1,0}^{(1)}\tilde{\eta}_{2,0}^{(1)}\tilde{\eta}_{1,0}^{(2)}\tilde{\eta}_{2,0}^{(2)}}\sinh\left(p_{1R}t + \tfrac{1}{2}\left(2\tilde{\tilde{\eta}}_{2,0}^{(k)} - 2\tilde{\tilde{\eta}}_{1,0}^{(\ell)} - \tilde{\tilde{\eta}}_{1,0}^{(1)} + \tilde{\tilde{\eta}}_{2,0}^{(2)} + \tilde{\tilde{\xi}}_{1,0} - \tilde{\tilde{\xi}}_{2,0}\right)\right)\Bigg], \end{aligned}$$

where $e^{\tilde{\tilde{\xi}}_{j,0}} = \tilde{\xi}_{j,0}$ and $e^{\tilde{\tilde{\eta}}_{j,0}^{(\ell)}} = \tilde{\eta}_{j,0}^{(\ell)}$ for $j = 1, 2$ and $\ell = 1, 2, \ldots, M$.

This double-pole M bright two-soliton solution contains $2M + 3$ real soliton parameters (i.e., $\tilde{\xi}_{j,0}$, p_{1R}, and $\tilde{\eta}_{j,0}^{(k)}$, with $j = 1, 2$ and $k = 1, 2, \ldots, M$) and M arbitrary nonlinearity coefficients (i.e., $\delta_1, \delta_2, \ldots, \delta_M$). The above double-pole M bright two-soliton solution is regular for the parameters satisfying the condition $\sum_{k=1}^{M} \delta_k \tilde{\eta}_{j,0}^{(k)2} > 0$ $(j = 1, 2)$. Here we wish to point out that for defocusing nonlinearity ($\delta_\ell < 0$), the regularity condition fails to hold and does not admit a double-pole M bright two-soliton. This statement is true for higher-order double-pole $2N$-solitons (with $N \geqslant 2$) too. However, for $\delta_\ell > 0$ or $\delta_\ell\delta'_\ell < 0$ ($\ell' \neq \ell$ and $\ell', \ell = 1, 2, \ldots, M$), which correspond to focusing and mixed (focusing-defocusing) nonlinearities, respectively, the regularity condition is satisfied and these result in the existence of smooth double-pole M bright two-solitons. Such a type of generalized double-pole soliton solutions have been reported for the focusing 2CNLS equations [i.e., $M = 2$, $\delta_1 > 0$, and $\delta_2 > 0$ in Eq. (1)] in Ref. [70] without much detail on their collision dynamics. Hereafter, we consider $\sum_{k=1}^{M} \delta_k \tilde{\eta}_{j,0}^{(k)2} > 0$ $(j = 1, 2)$ to avoid the singular double-pole two-soliton solutions and desist from discussing the double-pole solitons in the MCNLS system with defocusing nonlinearity ($\delta_\ell < 0$). It is worth noting that for $g^{(\ell)} = g^{(1)}\tilde{\eta}_{1,0}^{(\ell)}/\tilde{\eta}_{1,0}^{(1)}$ when $\tilde{\eta}_{2,0}^{(\ell)} = \kappa\tilde{\eta}_{1,0}^{(\ell)}$ (κ is an arbitrary nonzero constant), this double-pole two-soliton solution of the MCNLS equations (1) would reduce to the double-pole two-soliton solution of the scalar NLS equation [i.e., $M = 1$ in Eq. (1)], where the interesting energy-sharing collision is not possible.

Since the double-pole two-soliton solution is generated from the single-pole M bright two-soliton solution (A1), we can investigate the double-pole M bright two-soliton collision process from the single-pole M bright two-soliton collision process. The analysis of single-pole two bright two-soliton collisions is investigated in Appendix A. To be consistent with the single-pole M bright two-soliton, we designate the double-pole two-solitons as soliton 1 and soliton 2, which correspond to the soliton 1 and soliton 2 in the single-pole two-soliton discussed in Appendix A. The amplitudes of the double-pole two-soliton before and after collision are given as

$$\begin{aligned} \left|\tilde{A}_\ell^{(j)-}\right|^2 &= \frac{p_{1R}^2\tilde{\eta}_{j,0}^{(\ell)2}}{\sum_{k=1}^{M} \delta_k \tilde{\eta}_{j,0}^{(k)2}}, \\ \left|\tilde{A}_\ell^{(j)+}\right|^2 &= \tilde{T}_\ell^{(j)2}\left|\tilde{A}_\ell^{(j)-}\right|^2, \\ & j = 1, 2;\ \ell = 1, 2, \ldots, M. \end{aligned} \tag{7}$$

Here $\tilde{A}_\ell^{(j)-}$ and $\tilde{A}_\ell^{(j)+}$ denote the amplitude of soliton j of the double-pole two-soliton in the u_ℓ component before and after collision, respectively, and $\tilde{T}_\ell^{(j)}$ represents the transition amplitude of soliton j (=1, 2) in the u_ℓ component. Detailed derivations of $\tilde{A}_\ell^{(j)\pm}$ are given in Appendix A. The soliton transition amplitudes are found to be

$$\tilde{T}_\ell^{(1)2} = \frac{\tilde{\eta}_{2,0}^{(\ell)2}\sum_{k=1}^{M} \delta_k \tilde{\eta}_{1,0}^{(k)2}}{\tilde{\eta}_{1,0}^{(\ell)2}\sum_{k=1}^{M} \delta_k \tilde{\eta}_{2,0}^{(k)2}}, \quad \tilde{T}_\ell^{(2)2} = \frac{\tilde{\eta}_{1,0}^{(\ell)2}\sum_{k=1}^{M} \delta_k \tilde{\eta}_{2,0}^{(k)2}}{\tilde{\eta}_{2,0}^{(\ell)2}\sum_{k=1}^{M} \delta_k \tilde{\eta}_{1,0}^{(k)2}}. \tag{8}$$

From the expression of soliton amplitudes (7), we can deduce the following relations to identify the nature of

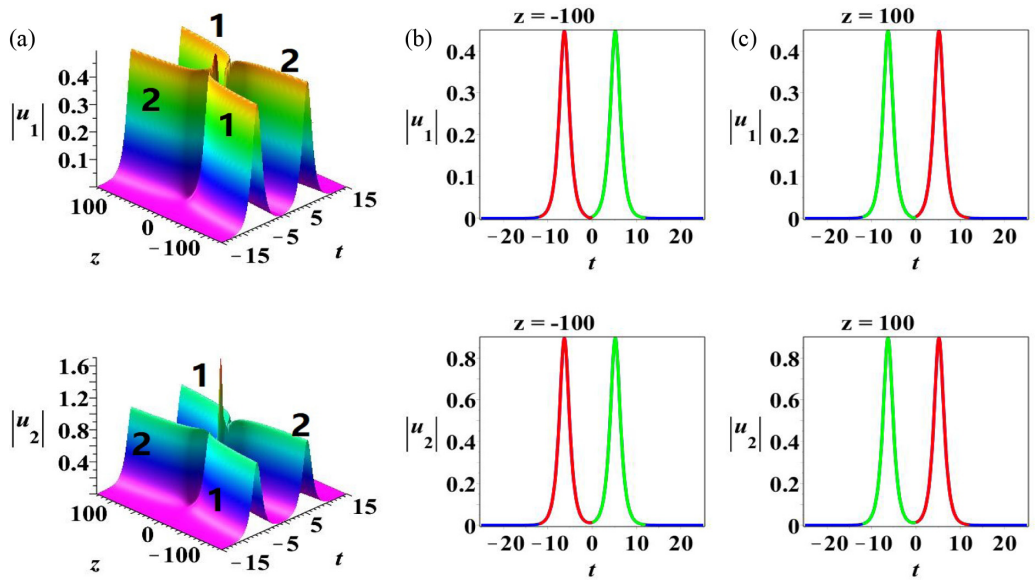

FIG. 1. (a) Elastic collision of the double-pole two bright two-solitons in the focusing 2CNLS equations (1) with the parameters $M = 2$, $\delta_1 = 1$, $\delta_2 = 1$, $\tilde{\xi}_{1,0} = -3$, $\tilde{\xi}_{2,0} = 1$, $\tilde{\eta}^{(1)}_{1,0} = 1$, $\tilde{\eta}^{(1)}_{2,0} = -1$, $\tilde{\eta}^{(2)}_{1,0} = 2$, $\tilde{\eta}^{(2)}_{2,0} = 2$, and $p_{1R} = 1$. Here we mark both solitons in the double-pole two-soliton as 1 and 2 for an easy understanding of the collision process. The intensity variations are shown clearly at (b) $z = -100$ (before collision) and (c) $z = 100$ (after collision) in soliton 1 (red line) and soliton 2 (green line).

collision:

$$\tilde{T}^{(1)}_{\ell}\tilde{T}^{(2)}_{\ell} = 1, \quad |\tilde{A}^{(2)+}_{\ell}| = |\tilde{A}^{(1)-}_{\ell}|, \quad |\tilde{A}^{(1)+}_{\ell}| = |\tilde{A}^{(2)-}_{\ell}|, \tag{9}$$

$$|\tilde{A}^{(1)-}_{\ell}|^2 + |\tilde{A}^{(2)-}_{\ell}|^2 = |\tilde{A}^{(1)+}_{\ell}|^2 + |\tilde{A}^{(2)+}_{\ell}|^2. \tag{10}$$

We list the physical consequences of the above mathematical expressions.

(i) From Eq. (9) one can obtain that $\tilde{T}^{(j)}_{\ell}$ can admit only two possible values, namely, $\tilde{T}^{(1)}_{\ell} = \tilde{T}^{(2)}_{\ell} = 1$, and $\tilde{T}^{(1)}_{\ell} > 1$ and $\tilde{T}^{(2)}_{\ell} < 1$ (or $\tilde{T}^{(1)}_{\ell} < 1$ and $\tilde{T}^{(2)}_{\ell} > 1$). When the transition amplitude $\tilde{T}^{(j)}_{\ell} = 1$, the collision between the double-pole bright two-soliton becomes elastic. This occurs only for a particular choice of parameters meeting the constraint $\sum_{k=1}^{M} \delta_k(\frac{\tilde{\eta}^{(k)2}_{2,0}}{\tilde{\eta}^{(\ell)2}_{2,0}} - \frac{\tilde{\eta}^{(k)2}_{1,0}}{\tilde{\eta}^{(\ell)2}_{1,0}}) = 0$. Furthermore, the special case $\tilde{T}^{(1)}_{1} = \tilde{T}^{(2)}_{1} = 1$ when $M = 1$ reminds us that the collision of the double-pole bright two-soliton is purely elastic as in the standard focusing NLS equation [i.e., $M = 1$ and $\delta_1 = 1$ in Eq. (1)]. Additionally, in a more general setting, the double-pole bright two-soliton undergoes the shape-changing (or energy-sharing) collision as $\tilde{T}^{(1)}_{\ell} > 1$ and $\tilde{T}^{(2)}_{\ell} < 1$ (or $\tilde{T}^{(1)}_{\ell} < 1$ and $\tilde{T}^{(2)}_{\ell} > 1$). In particular, the relations $|\tilde{A}^{(2)+}_{\ell}| = |\tilde{A}^{(1)-}_{\ell}|$ and $|\tilde{A}^{(1)+}_{\ell}| = |\tilde{A}^{(2)-}_{\ell}|$ indicate that the two solitons exchange their intensities exactly after collision. We call such a special shape-changing collision an energy-exchanging collision.

(ii) Next, Eq. (10) implies that the total intensity of both colliding solitons is conserved in each component u_{ℓ}. Furthermore, from Eq. (7) we can obtain the amplitudes of the double-pole two bright two-soliton before collision and after collision and the nonlinear coefficients satisfy the following relation:

$$\sum_{k=1}^{M} \delta_k |\tilde{A}^{(j)-}_{k}|^2 = \sum_{k=1}^{M} \delta_k |\tilde{A}^{(j)+}_{k}|^2 = p^2_{1R}, \quad j = 1, 2. \tag{11}$$

The above relation indicates that, for each soliton in the double-pole bright two-soliton, the total amplitude before or after collision in all components u_{ℓ} ($\ell = 1, 2, \ldots, M$) is only related to the parameter p_{1R} and the nonlinearity coefficients δ_k. In the mixed focusing-defocusing MCNLS equation, if for simplicity we take $\delta_1, \delta_2, \ldots, \delta_k > 0$ and $\delta_{k+1}, \ldots, \delta_M < 0$ in Eq. (1), the total amplitude of the focusing components is larger than the defocusing components when the absolute values of nonlinear coefficients are equal, namely, $\sum_{s=1}^{k} |\tilde{A}^{(j)\pm}_{s}|^2 > \sum_{s=k+1}^{M} |\tilde{A}^{(j)\pm}_{s}|^2$ when $|\delta_1| = |\delta_2| = \cdots = |\delta_M|$.

Figure 1 shows an elastic collision of the double-pole two bright two-soliton in the focusing 2CNLS equations [$M = 2$ and $\delta_1 = \delta_2 = 1$ in Eq. (1)], where the amplitudes of both solitons in the u_1 and u_2 components are $\frac{\sqrt{5}}{5}$ units and $\frac{2\sqrt{5}}{5}$ units, respectively, and remain the same before and after collision. Figures 2 and 3 show the interesting energy (intensity)-exchanging collisions of the double-pole two bright two-soliton for the focusing 2CNLS equations [$M = 2$, $\delta_1 = 1$, and $\delta_2 = 1$ in Eq. (1)] and the mixed focusing-defocusing 2CNLS equations [$M = 2$, $\delta_1 = 1$, and $\delta_2 = -1$ in Eq. (1)], respectively, for an easy understanding of the difference in the collision dynamics between the two models. We can see that these two solitons exactly exchange their intensities after collision such that the amplitude value of soliton 1 (soliton 2) after collision is equal to the amplitude value of soliton 2 (soliton 1) before collision in both focusing and mixed 2CNLS equations. However, the types of change in these two models are different due to the nature of nonlin-

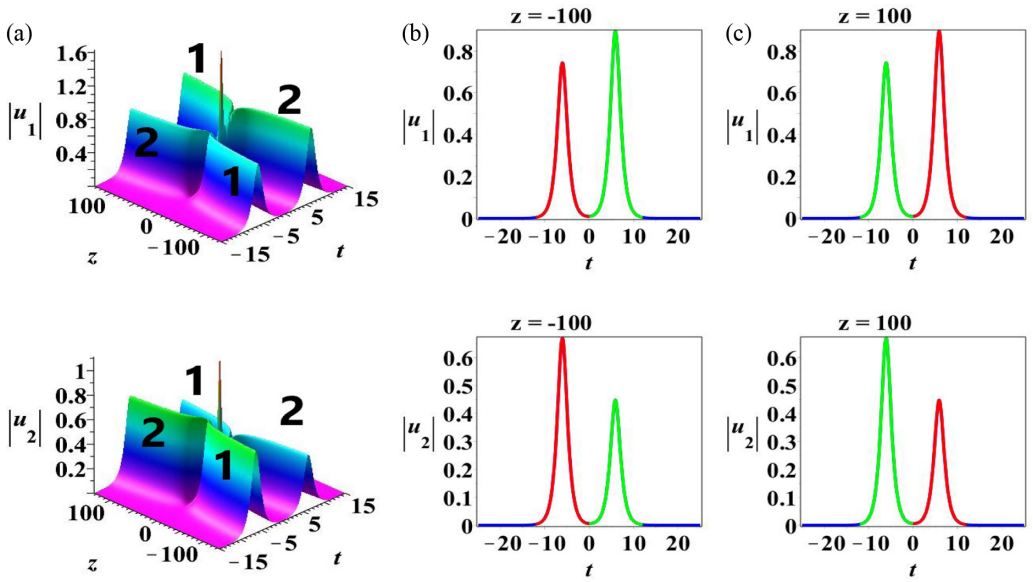

FIG. 2. (a) Energy-exchanging collisions of the double-pole two bright two-solitons in the focusing 2CNLS equations (1) with the parameters $M = 2$, $\delta_1 = 1$, $\delta_2 = 1$, $p_{1R} = 1$, $\tilde{\xi}_{1,0} = -\frac{29}{10}$, $\tilde{\xi}_{2,0} = 1$, $\tilde{\eta}^{(1)}_{1,0} = 2$, $\tilde{\eta}^{(1)}_{2,0} = 1$, $\tilde{\eta}^{(2)}_{1,0} = \frac{9}{5}$, and $\tilde{\eta}^{(2)}_{2,0} = \frac{1}{2}$. Here we mark the two solitons in the double-pole two-soliton as 1 and 2 in order to understand the energy-exchanging collision processes more clearly. The intensity exchange between the solitons is shown (b) before collision (at $z = -100$) and (c) after collision (at $z = 100$), with soliton 1 marked by the red line and soliton 2 by the green line.

earities (δ_ℓ). To be specific, a given soliton experiences the opposite intensity variation after collision between the two components in the focusing 2CNLS equations: The amplitude of soliton 1 increases after collision in the u_1 component, but its amplitude decreases in the u_2 component. In contrast to soliton 1, the amplitude of soliton 2 decreases after collision in the u_1 component, while it increases in the u_2 component. Such opposite changes in amplitude and intensity of solitons can be referred to as type-I energy-sharing collisions as in the case of standard or single-pole soliton collision dynamics [35], which is shown to be present or possible here in the double-pole bright soliton collision. Further, the intensity conservation is taking place in individual components apart from the conservation of the total intensity of double-pole solitons among all components for the MCNLS system with focusing nonlinearities. To elucidate the understanding, such a type-I

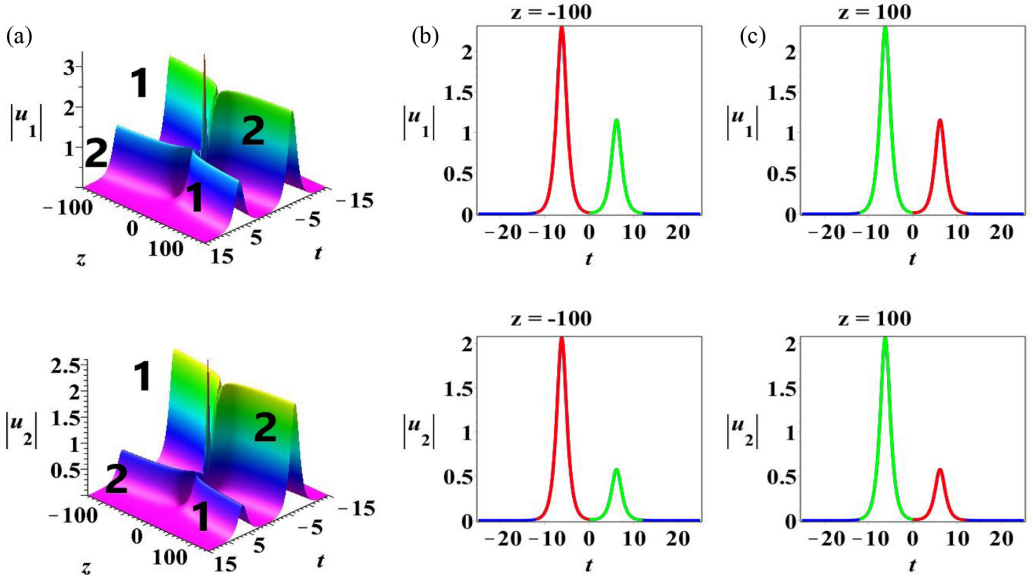

FIG. 3. (a) Energy-exchanging collisions of the double-pole two bright two-solitons in the mixed focusing-defocusing 2CNLS equations (1) with the parameters $M = 2$, $\delta_1 = 1$, $\delta_2 = -1$, $p_{1R} = 1$, $\tilde{\xi}_{1,0} = -\frac{11}{10}$, $\tilde{\xi}_{2,0} = 1$, $\tilde{\eta}^{(1)}_{1,0} = 2$, $\tilde{\eta}^{(1)}_{2,0} = 1$, $\tilde{\eta}^{(2)}_{1,0} = \frac{9}{5}$, and $\tilde{\eta}^{(2)}_{2,0} = \frac{1}{2}$. Here we mark the two solitons in the double-pole two-soliton as 1 and 2 in order to understand the energy-exchanging collision processes clearly. The intensity exchange between the solitons are shown (b) before collision (at $z = -100$) and (c) after collision (at $z = 100$), with soliton 1 marked by the red line and soliton 2 by the green line.

energy-sharing collision of double-pole solitons is shown in Fig. 2, where the amplitude of soliton 1 increases from $\frac{10\sqrt{181}}{181}$ units to $\frac{2\sqrt{5}}{5}$ units and that of soliton 2 decreases from $\frac{2\sqrt{5}}{5}$ units to $\frac{10\sqrt{181}}{181}$ units during the collision process in the u_1 component. The opposite type of change happens in the u_2 component, where the amplitude of soliton 1 decreases from $\frac{9\sqrt{181}}{181}$ units to $\frac{\sqrt{5}}{5}$ units and that of soliton 2 increases from $\frac{\sqrt{5}}{5}$ units to $\frac{9\sqrt{181}}{181}$ units.

On the other hand, one can note that the nature of sharing or exchange of intensity for a given soliton is the same in both components for the mixed focusing-defocusing 2CNLS equations. For example, the intensity of soliton 1 (soliton 2) decreases (increases) after collision in both the u_1 and u_2 components. Here the intensity is conserved in individual components separately in addition to the difference in intensities between the components, instead of the total intensity, due to the mixed type of nonlinearities ($\delta_1 > 0$ and $\delta_2 < 0$); such a scenario is referred to as type-II energy-sharing collision as in the standard single-pole collision [35]. This is demonstrated in Fig. 3, where the intensity of soliton 1 decreases from $\frac{10\sqrt{19}}{19}$ units to $\frac{2\sqrt{3}}{3}$ units and soliton 2 increases from $\frac{2\sqrt{3}}{3}$ units to $\frac{10\sqrt{19}}{19}$ units during the collision process in the u_1 (focusing) component. The change of the intensities in the u_2 (defocusing) component is also similar, but with different magnitudes, such that the intensity of soliton 1 decreases from $\frac{9\sqrt{19}}{19}$ units to $\frac{\sqrt{3}}{3}$ units and that of soliton 2 increases from $\frac{\sqrt{3}}{3}$ units to $\frac{9\sqrt{19}}{19}$ units, corresponding to mixed 2CNLS soliton collisions.

In these energy-exchanging collisions, the two bright solitons possessing unequal amplitudes before collision exchange their intensities after collision. This is a unique (but expected) phenomenon of the multicomponent NLS equations as compared with their single-component counterpart. A double-pole two-soliton in the standard scalar NLS equation was reported in [43] which undergoes only elastic collision without any change in amplitude before and after collision. We wish to stress that here we report the inelastic (shape-changing or energy-sharing) interaction of the bright double-pole solitons. Earlier in the literature such inelastic collisions were reported only for the standard (pairwise) collision of single-pole bright solitons. One can witness another important difference between the present double-pole and standard (single-pole) two-soliton energy-sharing collisions. In the standard two-soliton case, the intensity of a given soliton after collision need not be exactly the same as that of another soliton's intensity before collision (to be precise, it does not need to be the exact exchange of intensity). However, here in the present double-pole soliton collision, the amplitude or intensity is exactly exchanged such that $|A_\ell^{(2)+}| = |A_\ell^{(1)-}|$ and $|A_\ell^{(1)+}| = |A_\ell^{(2)-}|$. This can be viewed as the state of the first soliton before interaction being copied to the state of the second soliton after collision and vice versa. Further, by adjusting the additional parameters suitably, here the pairwise nature of collision can be transformed to single-point collision in the higher-order double-pole soliton interactions, which we will address in the forthcoming section. This process of single-point collision of multiple solitons can also be referred to as phase-synchronized soliton collisions.

B. Multiple double-pole M bright $2N$-solitons and collisions

The multiple (higher-order) double-pole M bright $2N$-soliton solution can be obtained by taking $N > 1$ in Eq. (4), which describes the collision of N pairs of double-pole two-solitons. The superposition of these N individual double-pole two-solitons can generate nontrivial wave patterns that are completely different from that of interacting $2N$-solitons, although this N double-pole soliton solution is generated from the $2N$-soliton solution.

To demonstrate the intricate behavior of such multiple double-pole bright $2N$-solitons ($N \geqslant 2$) in the MCNLS equations (1), we consider the double-pole four-solitons as an example. By taking $N = 2$ in Eq. (4), the functions f and $g^{(\ell)}$ of the double-pole four-soliton solution (3) can be expressed as

$$f = \begin{vmatrix} \tilde{m}_{1,1} & \tilde{m}_{1,2} & \tilde{m}_{1,3} & \tilde{m}_{1,4} \\ \tilde{m}_{2,1} & \tilde{m}_{2,2} & \tilde{m}_{2,3} & \tilde{m}_{2,4} \\ \tilde{m}_{3,1} & \tilde{m}_{3,2} & \tilde{m}_{3,3} & \tilde{m}_{3,4} \\ \tilde{m}_{4,1} & \tilde{m}_{4,2} & \tilde{m}_{4,3} & \tilde{m}_{4,4} \end{vmatrix},$$

$$g^{(\ell)} = \begin{vmatrix} \tilde{m}_{1,1} & \tilde{m}_{1,2} & \tilde{m}_{1,3} & \tilde{m}_{1,4} & \phi_1 \\ \tilde{m}_{2,1} & \tilde{m}_{2,2} & \tilde{m}_{2,3} & \tilde{m}_{2,4} & \phi_2 \\ \tilde{m}_{3,1} & \tilde{m}_{3,2} & \tilde{m}_{3,3} & \tilde{m}_{3,4} & \phi_3 \\ \tilde{m}_{4,1} & \tilde{m}_{4,2} & \tilde{m}_{4,3} & \tilde{m}_{4,4} & \phi_4 \\ i\tilde{\eta}_{1,0}^{(\ell)} & i\tilde{\eta}_{2,0}^{(\ell)} & i\tilde{\eta}_{3,0}^{(\ell)} & i\tilde{\eta}_{4,0}^{(\ell)} & 0 \end{vmatrix}, \tag{12}$$

where the matrix elements $\tilde{m}_{s,j}$ and ϕ_s are given below Eq. (4) for $s, j = 1, 2, 3, 4$. A categorical analysis of the collision process of the above double-pole bright four-solitons can be done along the lines of the double-pole bright two-soliton in such a way that the former is a superposition of the latter. Note that the transition amplitudes $\tilde{T}_\ell^{(j)}$ and $\tilde{T}_\ell^{(2+j)}$ admit the relation $\tilde{T}_\ell^{(2+j)} = 1/\tilde{T}_\ell^{(j)}$, where $j = 1, 2$. As a consequence, we obtain three types of double-pole four-soliton collisions for different choice combinations of the transition amplitudes $\tilde{T}_\ell^{(1)}$ and $\tilde{T}_\ell^{(2)}$: (i) elastic collisions, which require $\tilde{T}_\ell^{(1)} = 1$ and $\tilde{T}_\ell^{(2)} = 1$, where $\tilde{T}_\ell^{(1)} = \frac{\tilde{\eta}_{3,0}^{(\ell)2} \sum_{k=1}^{M} \delta_k \tilde{\eta}_{1,0}^{(k)2}}{\tilde{\eta}_{1,0}^{(\ell)2} \sum_{k=1}^{M} \delta_k \tilde{\eta}_{3,0}^{(k)2}}$ and $\tilde{T}_\ell^{(2)} = \frac{\tilde{\eta}_{4,0}^{(\ell)2} \sum_{k=1}^{M} \delta_k \tilde{\eta}_{2,0}^{(k)2}}{\tilde{\eta}_{2,0}^{(\ell)2} \sum_{k=1}^{M} \delta_k \tilde{\eta}_{4,0}^{(k)2}}$; (ii) energy-exchanging collisions, which take place for $\tilde{T}_\ell^{(1)} \neq 1$ and $\tilde{T}_\ell^{(2)} \neq 1$; and (iii) a mixture of elastic and energy-exchanging collisions for $\tilde{T}_\ell^{(1)} = 1$ and $\tilde{T}_\ell^{(2)} \neq 1$ or for $\tilde{T}_\ell^{(1)} \neq 1$ and $\tilde{T}_\ell^{(2)} = 1$. This implies that only two solitons can experience energy-exchanging collisions while the other two remain intact.

Figures 4–6 show these three types of double-pole four-soliton collisions. Figure 4 shows the elastic collision of double-pole four-solitons for the parameters $\tilde{\xi}_{k,0} = -3$, $\tilde{\xi}_{l,0} = 1$, $\tilde{\eta}_{k,0}^{(1)} = 1$, $\tilde{\eta}_{l,0}^{(1)} = -1$, $\tilde{\eta}_{k,0}^{(2)} = 2$, $\tilde{\eta}_{l,0}^{(2)} = 2$, $p_{1R} = 1$, and $p_{2R} = \frac{9}{10}$ ($k = 1, 2$ and $l = 3, 4$). This particular parameter choice also induces oscillations far from the interaction regime where four waves cross. Another important observation here is a special type of synchronization behavior. The four localized nonlinear waves arrive in a common phase at the interaction point, thereby producing a large-amplitude nonlinear

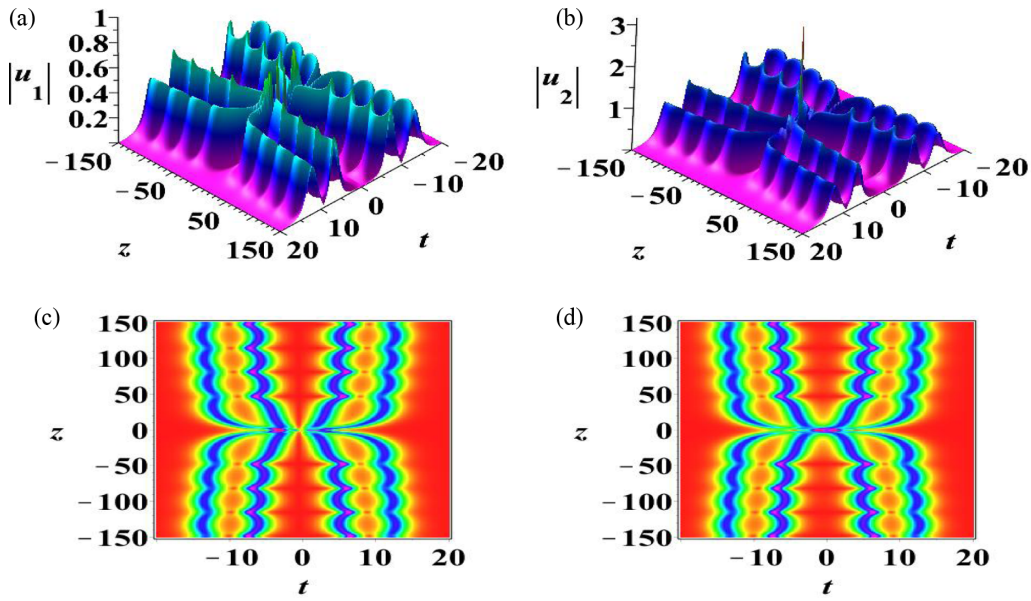

FIG. 4. (a) and (b) Elastic collisions of the double-pole bright four-soliton with oscillating patterns in the focusing 2CNLS equation (1) with the parameters $M = 2$, $\delta_1 = 1$, $\delta_2 = 1$, $\tilde{\xi}_{1,0} = -3$, $\tilde{\xi}_{2,0} = -3$, $\tilde{\xi}_{3,0} = 1$, $\tilde{\xi}_{4,0} = 1$, $\tilde{\eta}^{(1)}_{1,0} = 1$, $\tilde{\eta}^{(1)}_{2,0} = 1$, $\tilde{\eta}^{(1)}_{3,0} = -1$, $\tilde{\eta}^{(1)}_{4,0} = -1$, $\tilde{\eta}^{(2)}_{1,0} = 2$, $\tilde{\eta}^{(2)}_{2,0} = 2$, $\tilde{\eta}^{(2)}_{3,0} = 2$, $\tilde{\eta}^{(2)}_{4,0} = 2$, $p_{1R} = 1$, and $p_{2R} = \frac{9}{10}$. (c) and (d) Density plots of (a) and (b), respectively.

wave at that position. Afterward, they get separated and retain their original profile of periodically oscillating pairs of solitons. Further, the nonlinear wave appearing at the interaction regime or point admits a higher intensity in the second component than that of the first component. In fact, at the interaction junction, the u_2 component attains a very high amplitude which can exceed three units, whereas the u_1 component can have an intensity only below a single unit. By properly tuning the parameters, one can control the amplification of these synchronized structures.

Figure 5 displays the energy-exchanging collision of double-pole four-solitons, in which the two solitons of each double-pole two-soliton exchange their intensities after collision. Here too the synchronization process takes place as demonstrated in Fig. 4. This suggests that such a type of synchronization can be one of the physical mechanisms behind the sudden formation and disappearance of huge-amplitude nonlinear waves in different physical contexts such as ocean waves and nonlinear optics. Figure 6 displays the mixed-type collision scenario of the double-pole four-solitons, in which

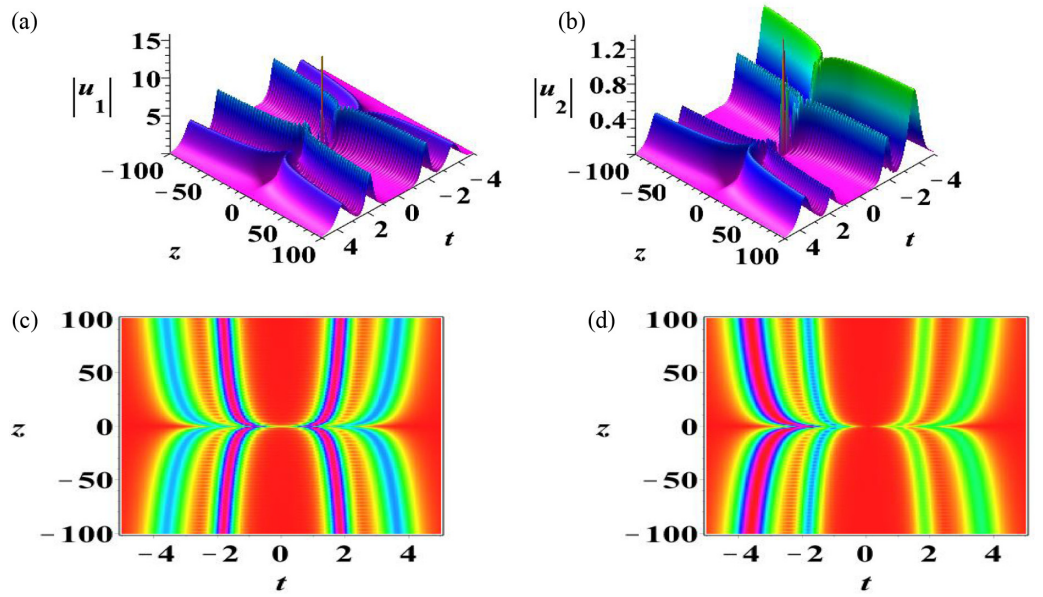

FIG. 5. (a) and (b) Energy-exchanging collisions of the double-pole bright four-solitons in the focusing 2CNLS equation (1) with the parameters $M = 2$, $\delta_1 = 1$, $\delta_2 = 1$, $\tilde{\xi}_{1,0} = \frac{199}{200}$, $\tilde{\xi}_{2,0} = \frac{599}{600}$, $\tilde{\xi}_{3,0} = 1$, $\tilde{\xi}_{4,0} = 1$, $\tilde{\eta}^{(1)}_{1,0} = 1$, $\tilde{\eta}^{(1)}_{2,0} = 1$, $\tilde{\eta}^{(1)}_{3,0} = -1$, $\tilde{\eta}^{(1)}_{4,0} = -1$, $\tilde{\eta}^{(2)}_{1,0} = \frac{1}{10}$, $\tilde{\eta}^{(2)}_{2,0} = \frac{1}{20}$, $\tilde{\eta}^{(2)}_{3,0} = \frac{1}{20}$, $\tilde{\eta}^{(2)}_{4,0} = \frac{1}{30}$, $p_{1R} = 5$, and $p_{2R} = 3$. (c) and (d) Density plots of (a) and (b), respectively.

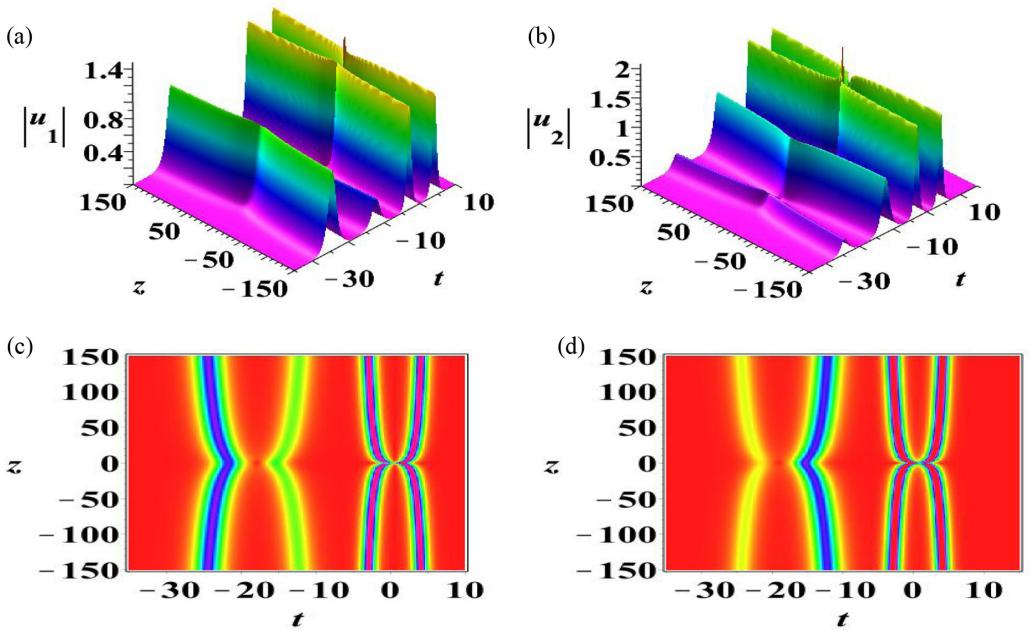

FIG. 6. (a) and (b) Mixture of energy-exchanging collision of the double-pole bright two-soliton and elastic collision of the double-pole bright two-soliton in the focusing 2CNLS equations (1) with the parameters $M = 2$, $\delta_1 = 1$, $\delta_2 = 1$, $\tilde{\xi}_{1,0} = -1.1 \times 10^{14}$, $\tilde{\xi}_{2,0} = -3$, $\tilde{\xi}_{3,0} = 1$, $\tilde{\xi}_{4,0} = 1$, $\tilde{\eta}^{(1)}_{1,0} = 10^6$, $\tilde{\eta}^{(1)}_{2,0} = 1$, $\tilde{\eta}^{(1)}_{3,0} = 10^7$, $\tilde{\eta}^{(1)}_{4,0} = -1$, $\tilde{\eta}^{(2)}_{1,0} = 10^7$, $\tilde{\eta}^{(2)}_{2,0} = 2$, $\tilde{\eta}^{(2)}_{3,0} = 10^7$, $\tilde{\eta}^{(2)}_{4,0} = 2$, $p_{1R} = 1$, and $p_{2R} = 2$. (c) and (d) Density plots of (a) and (b), respectively.

the two-soliton located around $t < -5$ [left pair in the two-dimensional density plot in Figs. 6(c) and 6(d)] experiences energy-exchanging collisions while the other two-soliton pair located around $t > -5$ [right pair in the two-dimensional density plot in Figs. 6(c) and 6(d)] displays mere elastic collisions in both components u_1 and u_2. These collision scenarios are applicable for the remaining components in the case of the MCNLS model. It should be noted that these second-order ($N = 2$) double-pole four-soliton collisions can be further extended to generalized multiple double-pole $2N$-soliton interactions with a synchronized phase resulting in a much-higher-amplitude and much-higher-intensity doubly localized wave at the point of collision, similar to the rogue wave with extreme amplitudes. Such a phase synchronized collision is one of the possible routes to achieve the generation of rogue waves and extreme waves with huge amplitudes, through multiple (double-pole or standard) soliton interactions. This can form another interesting study, but a more detailed investigation is beyond the scope of the present work.

III. MULTIPLE DOUBLE-POLE $M-1$ BRIGHT-DARK SOLITONS AND ENERGY-EXCHANGING COLLISION IN MCNLS EQUATIONS

In this section we intend to investigate the dynamics of multiple double-pole bright-dark $2N$-solitons for the MCNLS equations (1). As in the case of general multiple M bright double-pole $2N$-soliton solutions constructed from the standard M-component bright $2N$-soliton solutions, one can also obtain general multiple double-pole $M-1$ bright, one dark $2N$-soliton solutions from the standard $M-1$ bright, one dark $2N$-soliton solutions by taking the long-wave limiting procedure. The explicit form of such standard bright-dark K-soliton solutions along with all parameters is given in Appendix B. Indeed, in Eq. (B2), by choosing the parameters as

$$\begin{aligned} K &= 2N, \\ p_{N+s} &= -p_s, \\ e^{\xi_{j,0}} &= \tilde{\xi}_{j,0} p_{jI} e^{(\pi/2)i}, \\ e^{\eta^{(\ell)}_{j,0}} &= \tilde{\eta}^{(\ell)}_{j,0} p_{jI} e^{(\pi/2)i}, \\ \tilde{\xi}_{s,0}\tilde{\xi}_{N+s,0} - \frac{p^2_{sR}\sum_{k=1}^{M-1}\delta_k \tilde{\eta}^{(k)}_{s,0}\tilde{\eta}^{(k)}_{N+s,0}}{\delta_M - p^2_{sR}} &= 0 \end{aligned} \tag{13}$$

and then by considering the limits $p_{sI} \to 0$ for $s = 1, 2, \ldots, N$, the double-pole $M-1$ bright, one dark $2N$-soliton solutions to the MCNLS equations (1) can be deduced in the form

$$\begin{aligned} u_\ell &= e^{2i\delta_M z}\frac{g^{(\ell)}(t,z)}{f(t,z)}, \\ \ell &= 1, 2, \ldots, M-1, \\ u_M &= e^{2i\delta_M z}\frac{g^{(M)}(t,z)}{f(t,z)}, \end{aligned} \tag{14}$$

where

$$f = \begin{vmatrix} \hat{m}^{(0)}_{s,j} & \hat{m}^{(0)}_{s,N+j} \\ \hat{m}^{(0)}_{N+s,j} & \hat{m}^{(0)}_{N+s,N+j} \end{vmatrix}_{1\leqslant s,j\leqslant N},$$

$$g^{(\ell)} = \begin{vmatrix} \hat{m}^{(0)}_{s,j} & \hat{m}^{(0)}_{s,N+j} & \tilde{\phi}_s \\ \hat{m}^{(0)}_{N+s,j} & \hat{m}^{(0)}_{N+s,N+j} & \tilde{\phi}_{N+s} \\ i\hat{\eta}^{(\ell)}_{j,0} & i\hat{\eta}^{(\ell)}_{N+j,0} & 0 \end{vmatrix}_{1\leqslant s,j\leqslant N},$$

$$g^{(M)} = \begin{vmatrix} \hat{m}^{(1)}_{s,j} & \hat{m}^{(1)}_{s,N+j} \\ \hat{m}^{(1)}_{N+s,j} & \hat{m}^{(1)}_{N+s,N+j} \end{vmatrix}_{1\leqslant s,j\leqslant N}, \quad \ell = 1, 2, \ldots, M, \tag{15}$$

and the matrix elements are given by

$$\hat{m}^{(n)}_{s,j} = \frac{(-1)^n \tilde{\xi}_{s,0}\tilde{\xi}_{j,0} e^{(p_{sR}+p_{jR})t + i(p^2_{sR}-p^2_{jR})z}}{p_{sR}+p_{jR}} + \frac{\sum_{k=1}^{M-1} \delta_k \tilde{\eta}^{(k)}_{s,0}\tilde{\eta}^{(k)}_{j,0}}{(p_{sR}+p_{jR}) + \left(\frac{\delta_M}{p_{sR}} + \frac{\delta_M}{p_{jR}}\right)},$$

$$\hat{m}^{(n)}_{N+s,N+j} = -\frac{(-1)^n \tilde{\xi}_{N+s,0}\tilde{\xi}_{N+j,0} e^{-(p_{sR}+p_{jR})t + i(p^2_{sR}-p^2_{jR})z}}{p_{sR}+p_{jR}} - \frac{\sum_{k=1}^{M-1} \delta_k \tilde{\eta}^{(k)}_{N+s,0}\tilde{\eta}^{(k)}_{N+j,0}}{(p_{sR}+p_{jR}) + \left(\frac{\delta_M}{p_{sR}} + \frac{\delta_M}{p_{jR}}\right)}.$$

In addition,

$$\hat{m}^{(n)}_{s,N+j} = \frac{(-1)^n \tilde{\xi}_{s,0}\tilde{\xi}_{N+j,0} e^{(p_{sR}-p_{jR})t + i(p^2_{sR}-p^2_{jR})z}}{(p_{sR}-p_{jR})} + \frac{\sum_{k=1}^{M-1} \delta_k \tilde{\eta}^{(k)}_{s,0}\tilde{\eta}^{(k)}_{N+j,0}}{(p_{sR}-p_{jR}) + \left(\frac{\delta_M}{p_{sR}} - \frac{\delta_M}{p_{jR}}\right)},$$

$$\hat{m}^{(n)}_{N+s,j} = -\frac{(-1)^n \tilde{\xi}_{N+s,0}\tilde{\xi}_{j,0} e^{-(p_{sR}-p_{jR})t + i(p^2_{sR}-p^2_{jR})z}}{(p_{sR}-p_{jR})} - \frac{\sum_{k=1}^{M-1} \delta_k \tilde{\eta}^{(k)}_{N+s,0}\tilde{\eta}^{(k)}_{j,0}}{(p_{sR}-p_{jR}) + \left(\frac{\delta_M}{p_{sR}} - \frac{\delta_M}{p_{jR}}\right)}$$

for $s \neq j$ and

$$\hat{m}^{(n)}_{s,N+s} = \tilde{\xi}_{s,0}\tilde{\xi}_{N+s,0}\left(t + 2ip_{sR}z + \frac{n}{p_{sR}}\right),$$

$$\hat{m}^{(n)}_{N+j,j} = \tilde{\xi}_{N+j,0}\tilde{\xi}_{j,0}\left(t - 2ip_{jR}z - \frac{n}{p_{sR}}\right),$$

while $\tilde{\phi}_s$ and $\tilde{\phi}_{N+s}$ take the form as given below Eq. (4). Here p_{sR}, $\tilde{\xi}_{s,0}$, $\tilde{\eta}^{(\ell)}_{j,0}$, $\tilde{\xi}_{N+s,0}$, and $\tilde{\eta}^{(\ell)}_{N+j,0}$ are arbitrary real parameters for $\ell = 1, 2, \ldots, M-1$ and some of them have to satisfy the condition

$$\tilde{\xi}_{s,0}\tilde{\xi}_{N+s,0} - \frac{p^2_{sR}\sum_{k=1}^{M-1}\delta_k \tilde{\eta}^{(k)}_{s,0}\tilde{\eta}^{(k)}_{N+s,0}}{\delta_M - p^2_{sR}} = 0. \tag{16}$$

Note that the $M-1$ components admit bright solitons (u_ℓ for $\ell = 1, 2, \ldots, M-1$) and the u_Mth component corresponds to the dark solitons.

A. Double-pole bright-dark two-soliton and energy-exchanging collision

In this section we consider the double-pole $M-1$ bright, one dark two-soliton arising as in the above solution (14) and (15) to explain the simplest possible energy-sharing collision of the double-pole bright-dark two-soliton in the MCNLS equations (1). Such a first-order double-pole bright-dark two-soliton solution can be obtained from Eq. (15) with $N = 1$, and the determinant forms of functions f, $g^{(\ell)}$, and $g^{(M)}$ explicitly read

$$f = \begin{vmatrix} \hat{m}^{(0)}_{1,1} & \hat{m}^{(0)}_{1,2} \\ \hat{m}^{(0)}_{2,1} & \hat{m}^{(0)}_{2,2} \end{vmatrix},$$

$$g^{(\ell)} = \begin{vmatrix} \hat{m}^{(0)}_{1,1} & \hat{m}^{(0)}_{1,2} & \tilde{\phi}_1 \\ \hat{m}^{(0)}_{2,1} & \hat{m}^{(0)}_{2,2} & \tilde{\phi}_2 \\ i\hat{\eta}^{(\ell)}_{1,0} & i\hat{\eta}^{(\ell)}_{2,0} & 0 \end{vmatrix}, \tag{17}$$

$$g^{(M)} = \begin{vmatrix} \hat{m}^{(1)}_{1,1} & \hat{m}^{(1)}_{1,2} \\ \hat{m}^{(1)}_{2,1} & \hat{m}^{(1)}_{2,2} \end{vmatrix},$$

where $\hat{m}^{(n)}_{1,1} = \frac{(-1)^n \tilde{\xi}^2_{1,0} e^{2p_{1R}t}}{2p_{1R}} + \frac{\sum_{k=1}^{M-1}\delta_k \tilde{\eta}^{(k)2}_{1,0}}{2(p_{1R}+\frac{\delta_M}{p_{1R}})}$, $\hat{m}^{(n)}_{1,2} = \tilde{\xi}_{1,0}\tilde{\xi}_{2,0}(t + 2ip_{1R}z + \frac{n}{p_{1R}})$, $\hat{m}^{(n)}_{2,1} = \tilde{\xi}_{1,0}\tilde{\xi}_{2,0}(t - 2ip_{1R}z - \frac{n}{p_{1R}})$, $\hat{m}^{(n)}_{2,2} = \frac{(-1)^{n+1}\tilde{\xi}^2_{2,0}e^{2p_{1R}t}}{2p_{1R}} - \frac{\sum_{k=1}^{M-1}\delta_k \tilde{\eta}^{(k)2}_{2,0}}{2(p_{1R}+\frac{\delta_M}{p_{1R}})}$, $\tilde{\phi}_1 = i\tilde{\xi}_{1,0}e^{p_{1R}(t+ip_{1R}z)}$, and $\tilde{\phi}_2 = i\tilde{\xi}_{2,0}e^{-p_{1R}(t-ip_{1R}z)}$. This double-pole bright-dark two-soliton solution contains a sum of $3M+1$ real arbitrary parameters: $2M+1$ soliton parameters (p_{1R}, $\tilde{\xi}_{j,0}$, and $\tilde{\eta}^{(\ell)}_{j,0}$, with $j = 1, 2$ and $\ell = 1, 2, \ldots, M-1$) and M nonlinearity coefficients $(\delta_1, \delta_2, \ldots, \delta_M)$. As mentioned in Eq. (16), these parameters have to obey the parametric condition $\tilde{\xi}_{1,0}\tilde{\xi}_{2,0} - \frac{p^2_{1R}\sum_{k=1}^{M-1}\delta_k \tilde{\eta}^{(k)}_{1,0}\tilde{\eta}^{(k)}_{2,0}}{\delta_M - p^2_{1R}} = 0$.

This double-pole bright-dark two-soliton solution would be regular when the arbitrary parameters satisfy the condition $\sum_{k=1}^{M-1}\frac{\delta_k \tilde{\eta}^{(k)2}_{j,0}}{1+\frac{\delta_M}{p^2_{1R}}} > 0$ ($j = 1, 2$), which is considered for our further analysis and discussion to avoid singular solutions. Furthermore, by taking appropriate choices of the parameters $\tilde{\eta}^{(\ell)}_{j,0}$ and p_{1R}, this regularity condition can very well be satisfied for the MCNLS equations (1) for all three different types of nonlinearity coefficients, namely, the focusing [$\delta_k > 0$ in Eq. (1)], the defocusing [$\delta_k < 0$ in Eq. (1)], and the mixed focusing-defocusing [$\delta_k > 0$, $\delta_{k'} < 0$, and $k \neq k'$ in Eq. (1)] cases. This is a salient feature of the present general double-pole bright-dark soliton solution.

The double-pole bright-dark two-soliton solution describes different collision dynamics depending on the parameters $\tilde{\xi}_{1,0}$ and $\tilde{\xi}_{2,0}$ that are discussed below.

Case 1. The first type of collision results when the parameters $\tilde{\xi}_{1,0}$ and $\tilde{\xi}_{2,0}$ are finite; this can be achieved by choosing $p^2_{1R} \neq \delta_M$ [see Eq. (16)]. In this case, the collision process of the double-pole bright-dark two-soliton can be studied by using the asymptotic analysis of the bright-dark two-soliton collision provided in Appendix B. Equations (B10)–(B13), with the parameters as given in Eq. (13) with the limit $p_{1R} \to 0$, result in the relation between the intensities of the two interacting double-pole bright-dark solitons before and after collision

$$\begin{aligned} \left|\hat{\hat{A}}^{(j)-}_\ell\right|^2 &= \frac{(p^2_{1R}+\delta_M)\tilde{\eta}^{(\ell)2}_{j,0}}{\sum_{k=1}^{M-1}\delta_k \tilde{\eta}^{(k)2}_{j,0}}, \\ \left|\hat{\hat{A}}^{(j)+}_\ell\right|^2 &= \hat{\hat{T}}^{(j)2}_\ell \left|\hat{\hat{A}}^{(j)-}_\ell\right|^2, \\ \left|\hat{\hat{A}}^{(j)-}_M\right|^2 &= \left|\hat{\hat{A}}^{(j)+}_M\right|^2 = 0 \end{aligned} \tag{18}$$

for $\ell = 1, 2, \ldots, M-1$; $j = 1, 2$; and the soliton transition amplitudes

$$\hat{\hat{T}}_\ell^{(1)2} = \frac{\tilde{\eta}_{2,0}^{(\ell)2} \sum_{k=1}^{M-1} \delta_k \tilde{\eta}_{1,0}^{(k)2}}{\tilde{\eta}_{1,0}^{(\ell)2} \sum_{k=1}^{M-1} \delta_k \tilde{\eta}_{2,0}^{(k)2}}, \quad \hat{\hat{T}}_\ell^{(2)2} = \frac{\tilde{\eta}_{1,0}^{(\ell)2} \sum_{k=1}^{M-1} \delta_k \tilde{\eta}_{2,0}^{(k)2}}{\tilde{\eta}_{2,0}^{(\ell)2} \sum_{k=1}^{M-1} \delta_k \tilde{\eta}_{1,0}^{(k)2}}. \tag{19}$$

Here the double-pole bright two-soliton appears in u_ℓ ($\ell = 1, 2, \ldots, M-1$) components, while the double-pole dark two-soliton arises in the u_M component alone. These quantities imply the following features of the double-pole bright-dark two-soliton collision dynamics.

(i) For the u_M component, corresponding to double-pole dark two-soliton, the relation $|\hat{\hat{A}}_M^{(j)-}|^2 = |\hat{\hat{A}}_M^{(j)+}|^2$ indicates that the intensities of the double-pole dark two-soliton remain unchanged after collision, namely, the darkness of this dark two-soliton is invariant before and after collision. Hence, the double-pole dark two-soliton displays only elastic collision due to the identical transition amplitudes $\hat{\hat{T}}_M^{(1)} = \hat{\hat{T}}_M^{(2)} = 1$.

(ii) Except for the u_M component, all the remaining u_ℓ components admit double-pole bright two-solitons. Further, the relations explaining the collisions of the double-pole bright two-solitons given by Eqs. (9) and (10) still hold for the bright component u_ℓ ($\ell = 1, 2, \ldots, M-1$) in the double-pole bright-dark two-soliton case, namely,

$$\hat{\hat{T}}_\ell^{(1)} \hat{\hat{T}}_\ell^{(2)} = 1, \quad |\hat{\hat{A}}_\ell^{(2)+}| = |\hat{\hat{A}}_\ell^{(1)-}|, \quad |\hat{\hat{A}}_\ell^{(1)+}| = |\hat{\hat{A}}_\ell^{(2)-}|, \tag{20}$$

$$|\hat{\hat{A}}_\ell^{(1)-}|^2 + |\hat{\hat{A}}_\ell^{(2)-}|^2 = |\hat{\hat{A}}_\ell^{(1)+}|^2 + |\hat{\hat{A}}_\ell^{(2)+}|^2, \quad \ell = 1, 2, \ldots, M-1. \tag{21}$$

These relations indicate that the double-pole $M-1$ bright two-solitons also exhibit two-types of collisions: elastic collision for $\hat{\hat{T}}_\ell^{(j)} = 1$ and energy-exchanging collision for $\hat{\hat{T}}_\ell^{(j)} \neq 1$. In particular, when $M = 2$, we can obtain $\hat{\hat{T}}_1^{(1)} = \hat{\hat{T}}_1^{(2)} = 1$ due to the existence of bright solitons in only the u_1 component. Hence the double-pole bright-dark two-soliton in the 2CNLS equations only admits elastic collisions. From Eq. (18) we can infer that the nonlinearity coefficients of the dark-component (δ_M) directly and strongly influence the intensities of the double-pole bright solitons. In each bright component u_ℓ, the intensities of the double-pole bright solitons are larger for the positive nonlinearity coefficient of the dark component u_M (i.e., $\delta_M > 0$) than that of the negative nonlinearity coefficient (i.e., $\delta_M < 0$). Additionally, the total intensity of solitons j (=1, 2) arising among all the u_ℓ ($\ell = 1, 2, \ldots, M-1$) bright components obeys the relation

$$\sum_{k=1}^{M-1} \delta_k |\hat{\hat{A}}_k^{(j)-}|^2 = \sum_{k=1}^{M-1} \delta_k |\hat{\hat{A}}_k^{(j)+}|^2 = p_{1R}^2 + \delta_M, \quad j = 1, 2. \tag{22}$$

From this relation one can observe that the total intensity of the bright soliton j in all bright components is also strongly affected by the nonlinear coefficient δ_M of the dark component u_M. Additionally, this total intensity is very different from that of the double-pole bright soliton j in all components discussed in Sec. II, which is only related to the parameter p_{1R} and is independent of the nonlinear coefficients δ_ℓ [see Eq. (11)]. Furthermore, since the intensity of the double-pole dark two-soliton is a constant and independent of any parameters, the nonlinearity coefficients δ_ℓ ($\ell = 1, 2, \ldots, M-1$) of bright components u_ℓ do not affect the intensities of the double-pole dark two-soliton in the u_M component.

Figure 7 shows the double-pole bright-dark two-soliton for the defocusing 2CNLS equations (i.e., $M = 2$, $\delta_1 < 0$, and $\delta_2 < 0$). As discussed above, one can observe that the double-pole bright-dark two-soliton in the 2CNLS equations only admits elastic collisions. Thus both the bright and dark double-pole solitons appearing in the u_1 and u_2 components, respectively, retain their intensities and travel unaltered before and after collision. Indeed, from Eq. (18) with the parameters given in Fig. 7(a), one can calculate the intensity (darkness) of the bright (dark) two-soliton appearing in the u_1 (u_2) component as $\frac{\sqrt{5}}{3}$ (0). Here we note that the defocusing 2CNLS equations do not admit a regular multicomponent double-pole bright-two-soliton solution, which was discussed in Sec. II, and hence the energy-sharing collisions are not possible.

Figures 8 and 9 show the energy-exchanging collisions of double-pole bright-dark two-solitons for the focusing 3CNLS equations and the mixed focusing-defocusing 3CNLS equations, respectively, with same choice of parameters p_{1R}, $\xi_{2,0}$, and $\eta_{j,0}^{(k)}$ ($j, k = 1, 2$). We note that one can calculate the value of $\xi_{1,0}$ corresponding to Figs. 8 and 9 from Eq. (16), which results in different values due to the different choices of nonlinearity coefficients δ_3, even with the same choice of p_{1R}, $\xi_{2,0}$, and $\eta_{j,0}^{(k)}$. In these two figures and cases the nonlinearity coefficients of bright components (u_1 and u_2) are equal and positive (i.e., $\delta_1 = \delta_2 = 1$), while that of the dark component (u_3) is opposite, namely, $\delta_3 = 1$ in Fig. 8 (focusing 3CNLS) and $\delta_3 = -1$ in Fig. 9 (mixed 3CLNS). From Eq. (18) we can obtain the changes in intensities of the double-pole bright two-soliton in the focusing 3CNLS equations (i.e., in Fig. 8): The intensity of soliton 1 increases from $\frac{\sqrt{2}}{2}$ units to 2 units in the u_1 component and decreases from $\frac{3\sqrt{2}}{2}$ unit to 1 unit in the u_2 component, while the intensity of soliton 2 changes in the opposite manner in such a way that it decreases from 2 units to $\frac{\sqrt{2}}{2}$ units in the u_1 component and increases from 1 unit to $\frac{3\sqrt{2}}{2}$ units in the u_2 component. In the case of mixed focusing-defocusing 3CNLS equations, as shown in Fig. 9, the nature of the amplitude changes is similar to that of Fig. 8, but with different magnitudes: The intensity of soliton 1 increases from $\sqrt{\frac{3}{10}}$ units to $2\sqrt{\frac{3}{5}}$ units in the u_1 component and decreases from $3\sqrt{\frac{3}{10}}$ units to $\sqrt{\frac{3}{5}}$ units in the u_2 component, whereas the intensity of soliton 2 decreases from $2\sqrt{\frac{3}{5}}$ units to $\sqrt{\frac{3}{10}}$ units in the u_1 component and increases from $\sqrt{\frac{3}{5}}$ units to $3\sqrt{\frac{3}{10}}$ units in the u_2 component. Thus, we can understand that in these collision processes, the double-pole bright solitons 1 and 2 exactly exchange their intensities after collision in the bright components (i.e., u_1 and u_2), whereas the intensity of double-pole dark solitons remains unchanged in the u_3 component. To sum up, one can easily understand that the bright-dark double-pole two-solitons in MCNLS equations with $M \geqslant 3$ show energy-exchanging collisions in the u_ℓ ($\ell = 1, 2, \ldots, M-1$) bright components accompanied by elastic collision in the only dark (u_M) component.

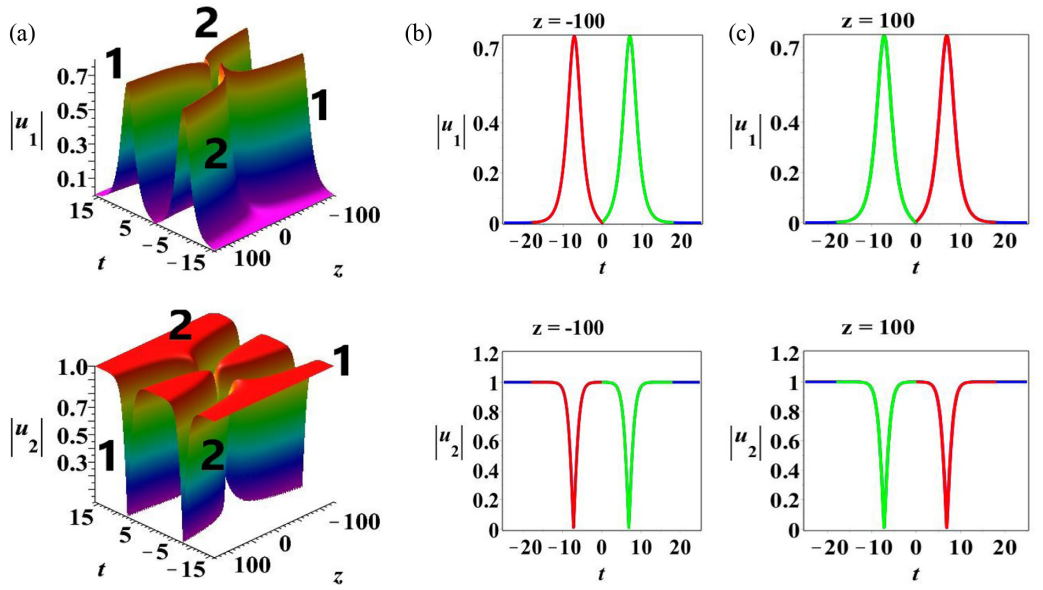

FIG. 7. (a) Elastic collision of the double-pole bright-dark two-soliton in the defocusing 2CNLS equations (1) with the parameters $M = 2$, $\delta_1 = -1$, $\delta_2 = -1$, $\tilde{\xi}_{1,0} = \frac{16}{13}$, $\tilde{\xi}_{2,0} = 2$, $\tilde{\eta}^{(1)}_{1,0} = 2$, $\tilde{\eta}^{(1)}_{2,0} = 4$, and $p_{1R} = \frac{2}{3}$. The intensity variations are shown at (b) $z = -100$ (before collision) and (c) $z = 100$ (after collision) in soliton 1 (red line) and soliton 2 (green line).

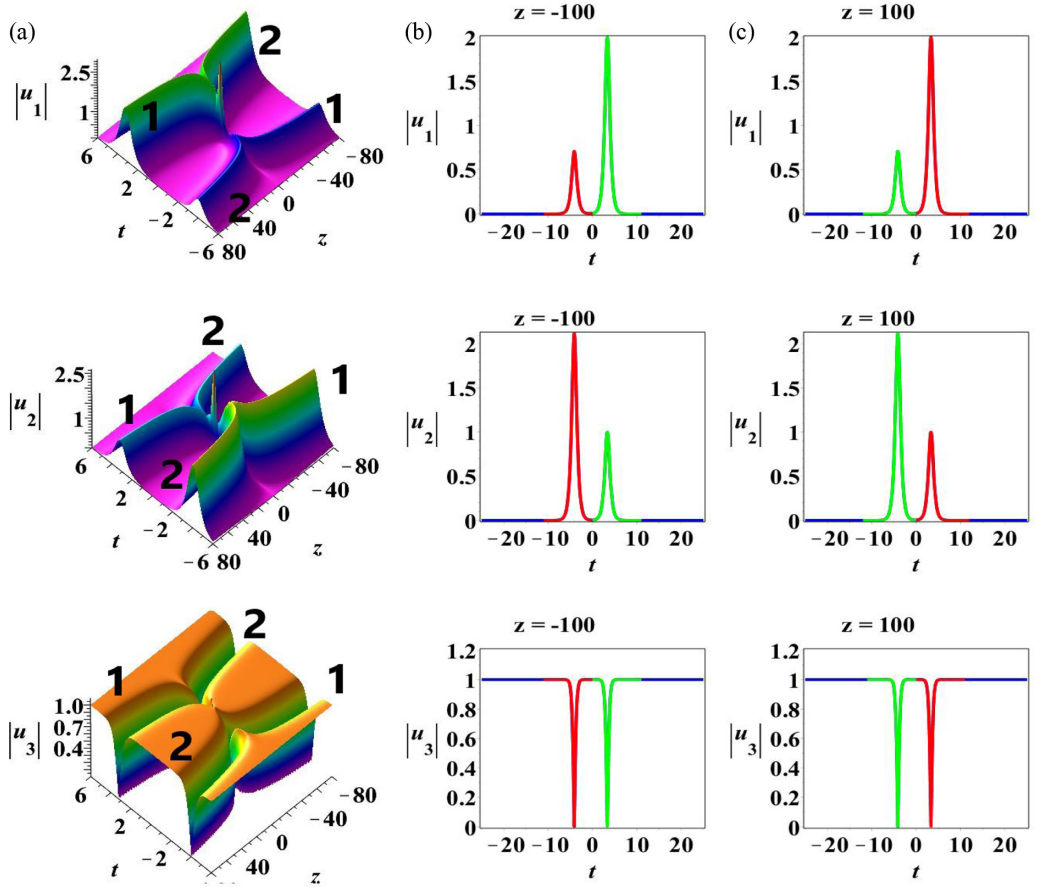

FIG. 8. (a) Energy-exchanging elastic collision of the double-pole bright-dark two-soliton in the focusing 3CNLS equations (1) with the parameters $M = 3$, $\delta_1 = 1$, $\delta_2 = 1$, $\delta_3 = 1$, $\tilde{\xi}_{1,0} = -\frac{20}{3}$, $\tilde{\xi}_{2,0} = 1$, $\tilde{\eta}^{(1)}_{1,0} = 1$, $\tilde{\eta}^{(1)}_{2,0} = 2$, $\tilde{\eta}^{(2)}_{1,0} = 3$, $\tilde{\eta}^{(2)}_{2,0} = 1$, and $p_{1R} = 2$. The intensity variations are shown clearly at (b) $z = -100$ (before collision) and (c) $z = 100$ (after collision) in soliton 1 (red line) and soliton 2 (green line).

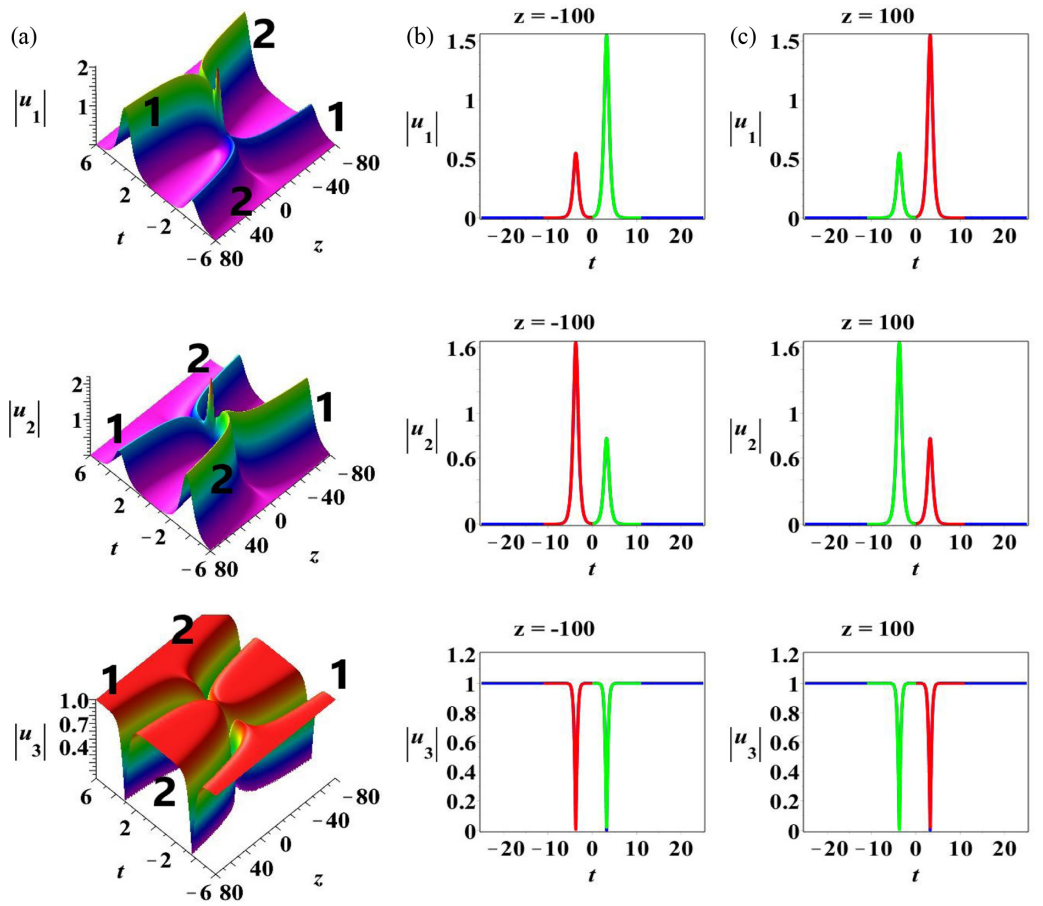

FIG. 9. (a) Energy-exchanging elastic collision of the double-pole bright-dark two-soliton in the mixed focusing-defocusing 3CNLS equation (1) with the parameters $M = 3$, $\delta_1 = 1$, $\delta_2 = 1$, $\delta_3 = -1$, $\tilde{\xi}_{1,0} = -4$, $\tilde{\xi}_{2,0} = 1$, $\tilde{\eta}^{(1)}_{1,0} = 1$, $\tilde{\eta}^{(1)}_{2,0} = 2$, $\tilde{\eta}^{(2)}_{1,0} = 3$, $\tilde{\eta}^{(2)}_{2,0} = 1$, and $p_{1R} = 2$. The intensity variations are shown at (b) $z = -100$ (before collision) and (c) $z = 100$ (after collision) in soliton 1 (red line) and soliton 2 (green line).

Case 2. A different class of collision features results when either of the parameters $\tilde{\xi}_{1,0}$ and $\tilde{\xi}_{2,0}$ approaches infinity (namely, either $\tilde{\xi}_1 \to \infty$ or $\tilde{\xi}_2 \to \infty$), which can be realized by taking $p^2_{1R} = \delta_M$ [see Eq. (13)]. When $\tilde{\xi}_j$ is finite and $\tilde{\xi}_{\tilde{j}} \to \infty$ ($j \neq \tilde{j} = 1, 2$), one can obtain from Eqs. (B5)–(B8) that $u^{(\tilde{j})\pm}_\ell \to 0$ and $u^{(j)\pm}_M \to e^{2i\delta_M z}$ for $\ell = 1, 2, \ldots, M-1$, which indicates that the soliton $\tilde{j}$ degenerates into the constant background, and the double-pole bright-dark soliton solution only consists of soliton j. In this case, the functions f, $g^{(\ell)}$, and $g^{(M)}$ of the double-pole bright-dark soliton solution can be written as

$$
\begin{aligned}
f &= -\frac{e^{(-1)^j 2p_{1R}t}}{4p^2_{1R}} \sum_{k=1}^{M-1} \frac{\delta_k \tilde{\eta}^{(k)2}_{j,0}}{1 + \frac{\delta_M}{p^2_{1R}}} - \tilde{\xi}^2_{j,0}\left(t^2 + 4p^2_{1R}z^2 + \frac{1}{4p^2_{1R}}\right), \\
g^{(\ell)} &= (-1)^j \tilde{\xi}_{j,0} \tilde{\eta}^{(\ell)}_{j,0}\left(2ip_{1R}z + (-1)^{j-1}t + \frac{1}{2p_{1R}}\right) e^{p_{1R}[ip_{1R}z + (-1)^j t]}, \\
g^{(M)} &= \frac{e^{(-1)^j 2p_{1R}t}}{4p^2_{1R}} \sum_{k=1}^{M-1} \frac{\delta_k \tilde{\eta}^{(k)2}_{j,0}}{1 + \frac{\delta_M}{p^2_{1R}}} - \tilde{\xi}^2_{j,0}\left[t^2 + \left(2p_{1R}z - \frac{i}{p_{1R}}\right)^2 + \frac{1}{4p^2_{1R}}\right].
\end{aligned}
\tag{23}
$$

Since such a double-pole bright-dark two-soliton solution is derived by taking $p^2_{1R} = \delta_M > 0$, the regularity condition becomes $\sum_{k=1}^{M-1} \delta_k \tilde{\eta}^{(k)2}_{j,0} > 0$ and the nonlinearity coefficient of the dark-component should be positive, namely, $\delta_M > 0$.

From the analysis of the double-pole bright-dark two-soliton solution with $\tilde{\xi}_{j,0}$ being finite and $\tilde{\xi}_{\tilde{j},0} \to \infty$ ($j \neq \tilde{j}$ and $j, \tilde{j} = 1, 2$), we can obtain the intensity of such a double-pole bright two-soliton in the u_ℓ ($\ell = 1, 2, \ldots,$

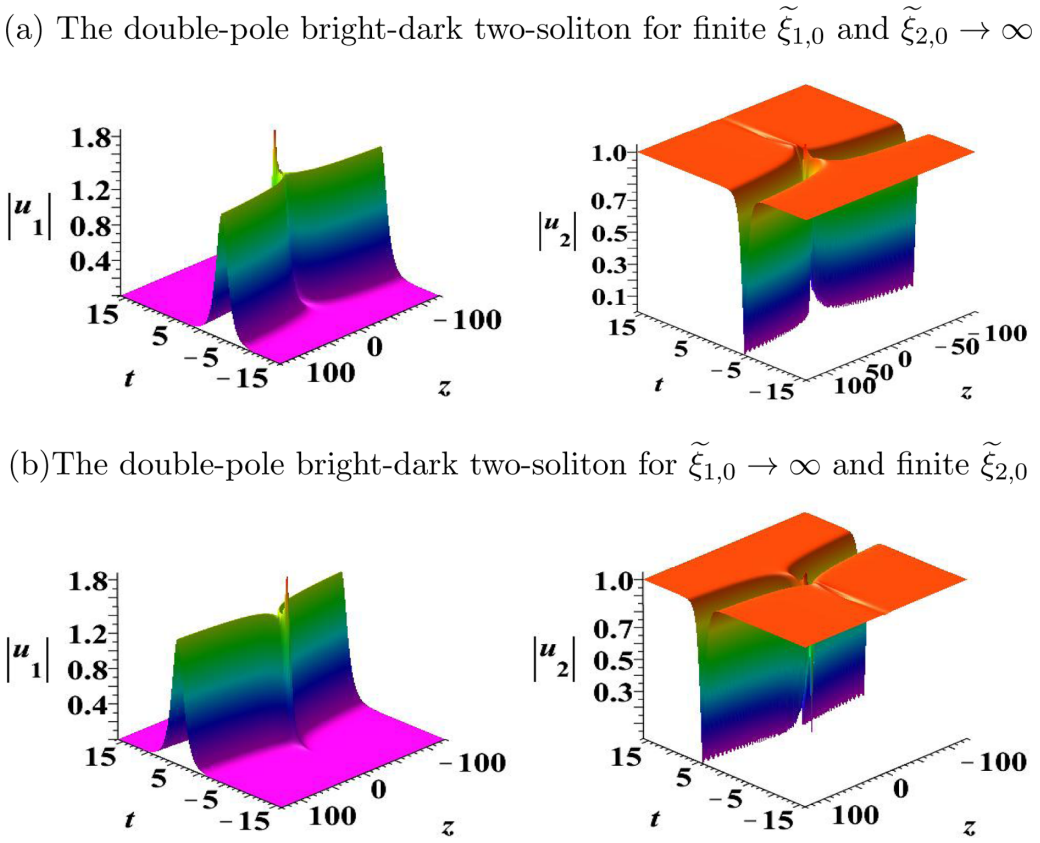

FIG. 10. Double-pole bright-dark two-soliton solution (17) in the focusing 2CNLS equations (1) with the parameters $M = 2$, $\delta_1 = 1$, $\delta_2 = 1$, and $p_{1R} = 1$. The case of $\tilde{\xi}_{1,0} = 1$ and $\tilde{\xi}_{2,0} \to \infty$ leads to soliton 2 degenerating into the (a) zero and (b) nonzero backgrounds and only soliton 1 exists on the background with parameters $\tilde{\eta}_{1,0}^{(1)} = 10$, $\tilde{\eta}_{2,0}^{(1)} = 1$. The case of $\tilde{\xi}_{1,0} \to \infty$ and $\tilde{\xi}_{2,0} = 1$ leads to soliton 1 disappearing into the (c) zero and (d) nonzero backgrounds and only soliton 2 propagates on the background with parameters $\tilde{\eta}_{1,0}^{(1)} = 1$, $\tilde{\eta}_{2,0}^{(1)} = 10$.

$M-1$) component as

$$|A_\ell^{(j)}|^2 = \frac{2\delta_M \tilde{\eta}_{j,0}^{(\ell)2}}{\sum_{k=1}^{M-1} \delta_k \tilde{\eta}_{j,0}^{(k)2}}. \tag{24}$$

However, the intensity or depth of the double-pole dark soliton in the dark component u_M approaches zero ($|A_M^{(j)}| \to 0$) on the constant nonvanishing background intensity of one unit. Figure 10 shows such collisions of double-pole bright-dark two-solitons in the defocusing 2CNLS equations for finite $\tilde{\xi}_{1,0}$ with $\tilde{\xi}_{2,0} \to \infty$ [Figs. 10(a) and 10(b)] and finite $\tilde{\xi}_{2,0}$ with $\tilde{\xi}_{1,0} \to \infty$ [Figs. 10(c) and 10(d)]. Thus, one can understand from this discussion and demonstrations that this double-pole bright-dark two-soliton is completely different from the double-pole bright-dark two-soliton arising when both $\tilde{\xi}_{j,0}$ and $\tilde{\xi}_{\tilde{j},0}$ are finite as shown in case 1 and through Figs. 6–9, where a pair of bright and dark solitons exists in a given u_ℓ component and u_M component, respectively, while the present double-pole bright-dark two-soliton contains only one soliton profile taking a curved path around $z \to 0$ as depicted in Fig. 10. To be precise, only soliton 1 exists and propagates on the zero (nonzero) background, while soliton 2 degenerates into the zero (nonzero) background in Fig. 10(a) [Fig. 10(b)]. In contrast, in Fig. 10(c) [Fig. 10(d)], soliton 2 only propagates on the zero (nonzero) background and soliton 1 disappears into the zero (nonzero) background. Additionally, we note that, since the regularity condition requires $\delta_1 > 0$ and $\delta_2 > 0$ for $M = 2$, only the focusing 2CNLS equations [i.e., $M = 2$, $\delta_1 > 0$, and $\delta_2 > 0$ in (1)] can feature such a regular double-pole bright-dark two-soliton solution, whereas the mixed focusing-defocusing 2CNLS equations [i.e., $M = 2$ and $\delta_1\delta_2 < 0$ in (1)] and the defocusing 2CNLS equations [i.e., $M = 2$, $\delta_1 < 0$, and $\delta_2 < 0$ in (1)] do not admit such regular bright-dark two-soliton structures. However, when $M > 2$, the regularity condition can be very well satisfied for $\delta_j > 0$ or $\delta_k\delta_j < 0$ ($k \neq j$ and $k, j = 1, 2, \ldots, M-1$) and such a regular double-pole bright-dark two-soliton exists in the focusing MCNLS system or in the mixed focusing-defocusing MCNLS system for $M \geqslant 3$.

In particular, when both parameters $\tilde{\xi}_{1,0}$ and $\tilde{\xi}_{2,0}$ approach infinity ($\tilde{\xi}_{1,0} \to \infty$ and $\tilde{\xi}_{2,0} \to \infty$), the double-pole bright-dark two-soliton solution (17) becomes

$$\begin{aligned} u_\ell &= 0, \\ \ell &= 1, 2, \ldots, M-1, \\ u_M &= e^{2i\delta_M z}\left(1 - \frac{4(4iz+1)}{4t^2 + 16z^2 + 1}\right). \end{aligned} \tag{25}$$

This represents that the double-pole soliton in the bright component u_ℓ completely degenerates to the zero background, while the dark component u_M gets shaped as an interesting

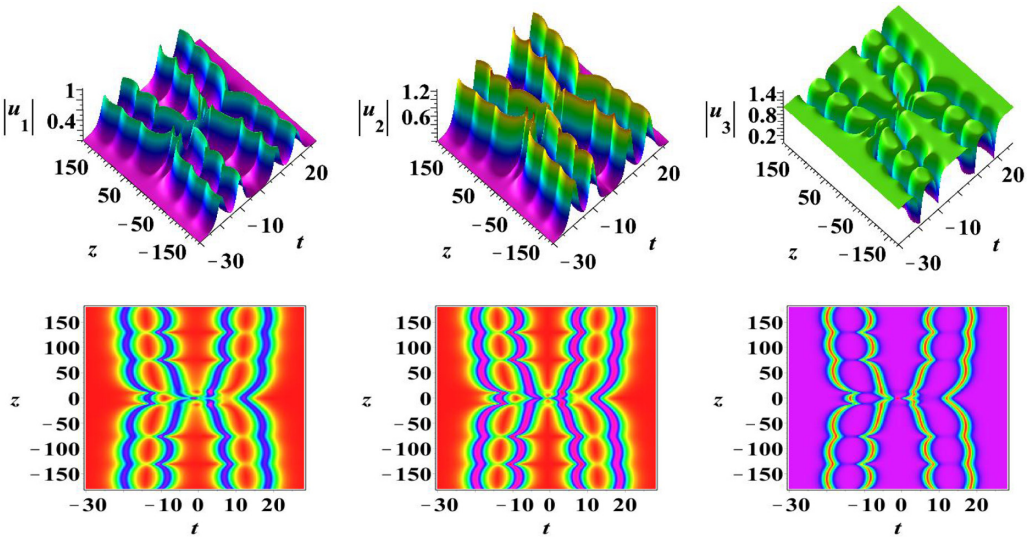

FIG. 11. The top row shows the elastic collision of the double-pole bright-dark four-soliton in the focusing 3NLS equation (1) with the parameters $M = 3$, $\delta_1 = 1$, $\delta_2 = 1$, $\delta_3 = 1$, $\tilde{\xi}_{1,0} = \frac{12}{5}$, $\tilde{\xi}_{2,0} = \frac{27}{7}$, $\tilde{\xi}_{3,0} = 1$, $\tilde{\xi}_{4,0} = 1$, $\tilde{\eta}^{(1)}_{1,0} = 1$, $\tilde{\eta}^{(1)}_{2,0} = 1$, $\tilde{\eta}^{(1)}_{3,0} = -1$, $\tilde{\eta}^{(1)}_{4,0} = -1$, $\tilde{\eta}^{(2)}_{1,0} = 2$, $\tilde{\eta}^{(2)}_{2,0} = 2$, $\tilde{\eta}^{(2)}_{3,0} = 2$, $\tilde{\eta}^{(2)}_{4,0} = 2$, $p_{1R} = \frac{2}{3}$, and $p_{2R} = \frac{3}{4}$. The bottom row is the density plot of the top row.

Peregrine soliton (i.e., fundamental rogue wave solution). This feature indicates that the collision of the double-pole two-soliton can generate a rogue wave, an alternate mechanism to achieve rogue waves, which has been an exciting notion of research in recent years. Proceeding further, one can look for the generation of such rogue waves during the collision of multiple double-pole solitons as well.

B. Multiple double-pole bright-dark solitons and their collisions

The multiple double-pole bright-dark soliton solution describes the superposition of several individual double-pole bright-dark two-solitons, which are generated from Eq. (15) with $N \geqslant 2$. Our analysis of the dynamics of the double-pole bright-dark two-soliton reveals that the multiple double-pole bright-dark $2N$-soliton possesses three different dynamical behaviors under different parametric conditions: (i) the existence of $2N$ soliton wave profiles for $\xi_{j,0} \neq \infty$ and $\xi_{N+j,0} \neq \infty$ $(1 \leqslant j \leqslant N)$, (ii) the presence of $2N-1$ soliton wave profiles for $\xi_{j,0} \to \infty$ or $\xi_{N+j,0} \to \infty$, and (iii) the coexistence of $2(N-1)$ soliton waves with a Peregrine soliton for $\xi_{j,0} \to \infty$ and $\xi_{N+j,0} \to \infty$.

To demonstrate the multiple double-pole bright-dark $2N$-soliton solutions, we consider the bright-dark four-soliton as an example; this can be obtained from Eqs. (14) and (15) by taking $N = 2$. The determinant forms of the functions f, $g^{(\ell)}$,

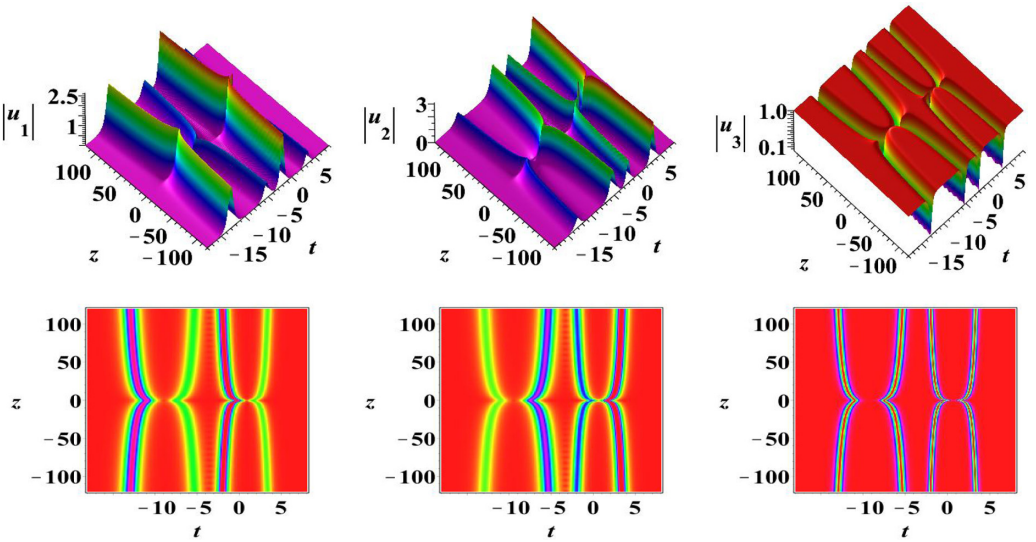

FIG. 12. The top row shows the energy-exchanging collision of the double-pole bright-dark four-soliton in the focusing 3-NLS equation (1) with the parameters $M = 3$, $\delta_1 = 1$, $\delta_2 = 1$, $\delta_3 = 1$, $\tilde{\xi}_{1,0} = -\frac{44}{3} \times 10^{12}$, $\tilde{\xi}_{2,0} = -\frac{51}{160}$, $\tilde{\xi}_{3,0} = 1$, $\tilde{\xi}_{4,0} = 1$, $\tilde{\eta}^{(1)}_{1,0} = 10^6$, $\tilde{\eta}^{(1)}_{2,0} = \frac{1}{20}$, $\tilde{\eta}^{(1)}_{3,0} = 10^7$, $\tilde{\eta}^{(1)}_{4,0} = -1$, $\tilde{\eta}^{(2)}_{1,0} = 10^6$, $\tilde{\eta}^{(2)}_{2,0} = \frac{1}{3}$, $\tilde{\eta}^{(2)}_{3,0} = 10^6$, $\tilde{\eta}^{(2)}_{4,0} = 1$, $p_{1R} = 2$, and $p_{2R} = 3$. The bottom row is the density plot of the top row.

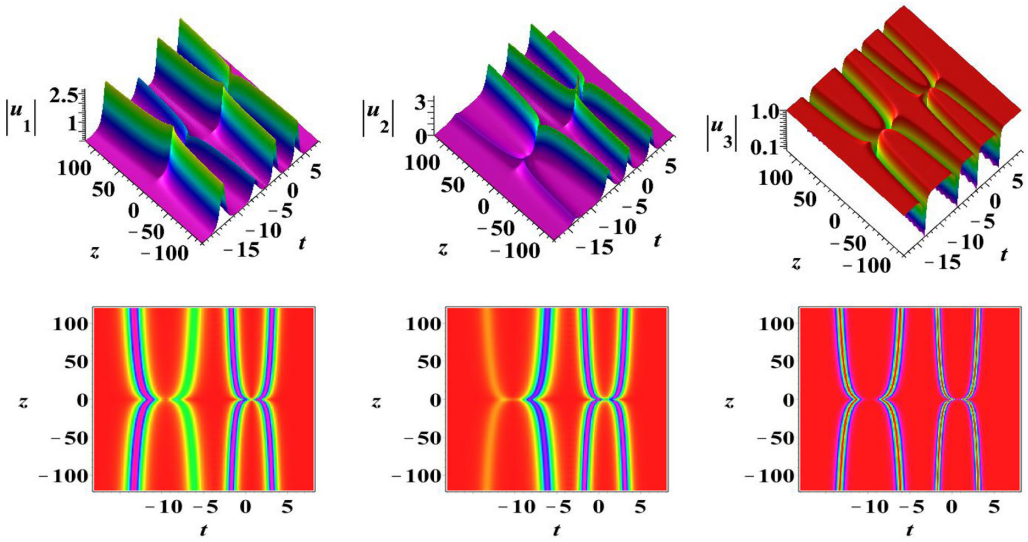

FIG. 13. The top row shows the energy-exchanging collision of the double-pole bright-dark four-soliton in the focusing 3NLS equation (1) with the parameters $M = 3$, $\delta_1 = 1$, $\delta_2 = 1$, $\delta_3 = 1$, $\tilde{\xi}_{1,0} = \frac{64}{75}$, $\tilde{\xi}_{2,0} = \frac{891}{800}$, $\tilde{\xi}_{3,0} = 1$, $\tilde{\xi}_{4,0} = 1$, $\tilde{\eta}^{(1)}_{1,0} = 1$, $\tilde{\eta}^{(1)}_{2,0} = 1$, $\tilde{\eta}^{(1)}_{3,0} = -1$, $\tilde{\eta}^{(1)}_{4,0} = -1$, $\tilde{\eta}^{(2)}_{1,0} = 2$, $\tilde{\eta}^{(2)}_{2,0} = \frac{1}{5}$, $\tilde{\eta}^{(2)}_{3,0} = \frac{1}{10}$, $\tilde{\eta}^{(2)}_{4,0} = \frac{1}{20}$, $p_{1R} = 4$, and $p_{2R} = 3$. The bottom row is the density plot of the top row.

and $g^{(M)}$ of the double-pole bright-dark four-soliton solution can be written explicitly as

$$f = \begin{vmatrix} \hat{m}^{(0)}_{1,1} & \hat{m}^{(0)}_{1,2} & \hat{m}^{(0)}_{1,3} & \hat{m}^{(0)}_{1,4} \\ \hat{m}^{(0)}_{2,1} & \hat{m}^{(0)}_{2,2} & \hat{m}^{(0)}_{2,3} & \hat{m}^{(0)}_{2,4} \\ \hat{m}^{(0)}_{3,1} & \hat{m}^{(0)}_{3,2} & \hat{m}^{(0)}_{3,3} & \hat{m}^{(0)}_{3,4} \\ \hat{m}^{(0)}_{4,1} & \hat{m}^{(0)}_{4,2} & \hat{m}^{(0)}_{4,3} & \hat{m}^{(0)}_{4,4} \end{vmatrix},$$

$$g^{(M)} = \begin{vmatrix} \hat{m}^{(1)}_{1,1} & \hat{m}^{(1)}_{1,2} & \hat{m}^{(1)}_{1,3} & \hat{m}^{(1)}_{1,4} \\ \hat{m}^{(1)}_{2,1} & \hat{m}^{(1)}_{2,2} & \hat{m}^{(1)}_{2,3} & \hat{m}^{(1)}_{2,4} \\ \hat{m}^{(1)}_{3,1} & \hat{m}^{(1)}_{3,2} & \hat{m}^{(1)}_{3,3} & \hat{m}^{(1)}_{3,4} \\ \hat{m}^{(1)}_{4,1} & \hat{m}^{(1)}_{4,2} & \hat{m}^{(1)}_{4,3} & \hat{m}^{(1)}_{4,4} \end{vmatrix}, \tag{26}$$

$$g^{(\ell)} = \begin{vmatrix} \hat{m}^{(0)}_{1,1} & \hat{m}^{(0)}_{1,2} & \hat{m}^{(0)}_{1,3} & \hat{m}^{(0)}_{1,4} & \tilde{\phi}_1 \\ \hat{m}^{(0)}_{2,1} & \hat{m}^{(0)}_{2,2} & \hat{m}^{(0)}_{2,3} & \hat{m}^{(0)}_{2,4} & \tilde{\phi}_2 \\ \hat{m}^{(0)}_{3,1} & \hat{m}^{(0)}_{3,2} & \hat{m}^{(0)}_{3,3} & \hat{m}^{(0)}_{3,4} & \tilde{\phi}_3 \\ \hat{m}^{(0)}_{4,1} & \hat{m}^{(0)}_{4,2} & \hat{m}^{(0)}_{4,3} & \hat{m}^{(0)}_{4,4} & \tilde{\phi}_4 \\ i\hat{\eta}^{(\ell)}_{1,0} & i\hat{\eta}^{(\ell)}_{2,0} & i\hat{\eta}^{(\ell)}_{3,0} & i\hat{\eta}^{(\ell)}_{4,0} & 0 \end{vmatrix},$$

$$\ell = 1, 2, \ldots, M,$$

where the matrix elements $\hat{m}^{(n)}_{s,j}$ ($n = 0$, 1 and s, $j = 1, 2, 3, 4$) take the form as given below Eq. (15). This bright-dark four-soliton solution contains $4M + 2$ soliton parameters (i.e., $\tilde{\xi}_{j,0}$, $\tilde{\eta}^{(\ell)}_{j,0}$, p_{1R}, and p_{2R}) and M is the number of nonlinearity coefficients ($\delta_1, \delta_2, \ldots, \delta_M$) among which the parameters $\tilde{\xi}_{1,0}$, $\tilde{\eta}^{(\ell)}_{1,0}$, $\tilde{\xi}_{3,0}$, $\tilde{\eta}^{(\ell)}_{3,0}$, and p_{1R} mainly control one double-pole two-soliton, while the remaining parameters (i.e., $\tilde{\xi}_{2,0}$, $\tilde{\eta}^{(\ell)}_{2,0}$, $\tilde{\xi}_{4,0}$, $\tilde{\eta}^{(\ell)}_{4,0}$, and p_{2R}) determine the nature of other double-pole two-solitons. For appropriate choices of $\tilde{\xi}_{j,0}$ ($j = 1, 2, 3, 4$) the double-pole bright-dark four-soliton describes three different dynamical behaviors during collision as discussed below.

Case 1. When all $\tilde{\xi}_{j,0}$ ($j = 1, 2, 3, 4$) are finite, the double-pole four-soliton solution results in the four-soliton excitations. In this case, the double-pole four-soliton in the dark component u_M only reveals elastic collision, whereas the double-pole four-soliton in the bright components u_ℓ ($\ell = 1, 2, \ldots, M-1$) can exhibit three different types of collision under different parametric conditions: (i) elastic collision for $\hat{\tilde{T}}^{(1)}_\ell = 1$ and $\hat{\tilde{T}}^{(2)}_\ell = 1$, where $\hat{\tilde{T}}^{(1)}_\ell = \frac{\tilde{\eta}^{(\ell)2}_{3,0} \sum_{k=1}^{M-1} \delta_k \tilde{\eta}^{(k)2}_{1,0}}{\tilde{\eta}^{(\ell)2}_{1,0} \sum_{k=1}^{M-1} \delta_k \tilde{\eta}^{(k)2}_{3,0}}$ and $\hat{\tilde{T}}^{(2)}_\ell = \frac{\tilde{\eta}^{(\ell)2}_{4,0} \sum_{k=1}^{M-1} \delta_k \tilde{\eta}^{(k)2}_{2,0}}{\tilde{\eta}^{(\ell)2}_{2,0} \sum_{k=1}^{M-1} \delta_k \tilde{\eta}^{(k)2}_{4,0}}$; (ii) energy-exchanging collision for $\hat{\tilde{T}}^{(1)}_\ell \neq 1$ and $\hat{\tilde{T}}^{(2)}_\ell \neq 1$; and (iii) a mixture of energy-exchanging and elastic collisions for $\hat{\tilde{T}}^{(1)}_\ell = 1$ and $\hat{\tilde{T}}^{(2)}_\ell \neq 1$ or for $\hat{\tilde{T}}^{(1)}_\ell \neq 1$ and $\hat{\tilde{T}}^{(2)}_\ell = 1$. Since $\hat{\tilde{T}}^{(3)}_\ell = 1/\hat{\tilde{T}}^{(1)}_\ell$ and $\hat{\tilde{T}}^{(4)}_\ell = 1/\hat{\tilde{T}}^{(2)}_\ell$, we do not list the expressions of $\hat{\tilde{T}}^{(3)}_\ell$ and $\hat{\tilde{T}}^{(4)}_\ell$ in the above parametric conditions. These three collision scenarios of double-pole bright four-solitons are very similar to that of multicomponent double-pole bright four-solitons discussed in the preceding section, except for their existence in $M - 1$ components here. Figure 11 displays the elastic collision of the double-pole four-soliton. It is quite evident that the collision of the four-solitons would generate periodic line waves in the interaction region. Figure 12 portrays the energy-exchanging collision of the double-pole four-soliton, where the two-soliton waves of each two-soliton exchange their intensities after collision. However, one can witness that the combination of elastic collision and the energy-exchanging collision of double-pole four-solitons takes place as shown in Fig. 13, where the double-pole two-solitons located around $t < -3$ exchange their intensities after collision, while other double-pole two-solitons located around $t > -3$ retain their intensities and reemerge unchanged after collision.

Case 2. When $\tilde{\xi}_{j,0} \to \infty$ and $\tilde{\xi}_{s,0}$ are finite (for $s = 1$ or 3 and $j = 2, 4$) or $\tilde{\xi}_{j,0}$ are finite and $\tilde{\xi}_{s,0} \to \infty$ (for $j = 1, 3$ and $s = 2$ or 4), the resulting double-pole four-soliton consists of only three-soliton waves and the fourth soliton vanishes or degenerates. Figure 14 shows the case of $\tilde{\xi}_{1,0} \to \infty$ and finite $\tilde{\xi}_{l,0}$ ($l = 2, 3, 4$). One can notice that the two-soliton

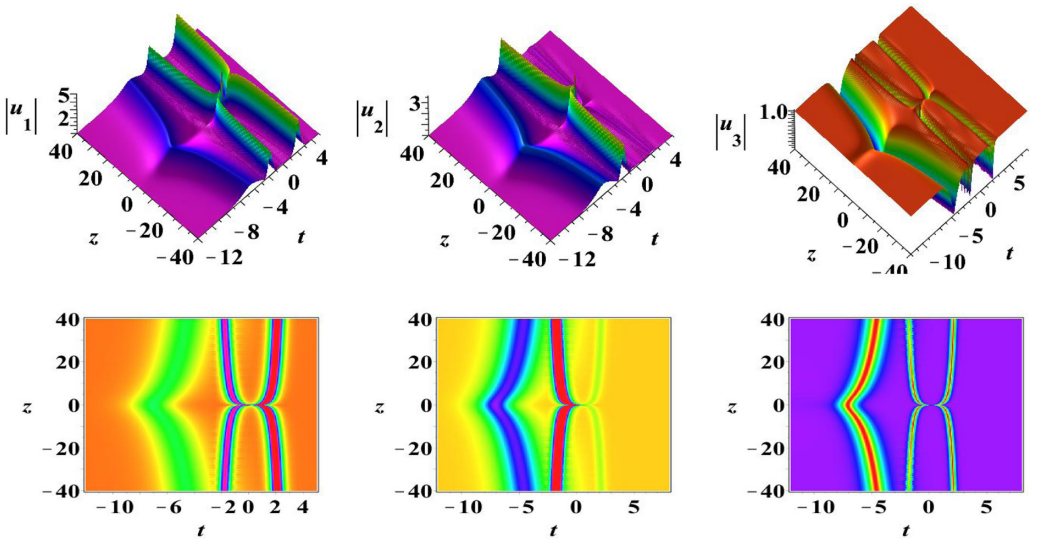

FIG. 14. The top row shows the double-pole bright-dark four-soliton in the focusing 3NLS equation (1) with the parameters $M = 3$, $\delta_1 = 1$, $\delta_2 = 1$, $\delta_3 = 1$, $\tilde{\xi}_{2,0} = -\frac{16}{5}$, $\tilde{\xi}_{3,0} = 3$, $\tilde{\xi}_{4,0} = 1$, $\tilde{\eta}^{(1)}_{2,0} = 1$, $\tilde{\eta}^{(1)}_{3,0} = 10^4$, $\tilde{\eta}^{(1)}_{4,0} = 2$, $\tilde{\eta}^{(2)}_{2,0} = 1$, $\tilde{\eta}^{(2)}_{3,0} = 10^4$, $\tilde{\eta}^{(2)}_{4,0} = 1$, $p_{1R} = 1$, and $p_{2R} = 4$. The bottom row is the density plot of the top row.

determined by the parameters $\tilde{\eta}^{(\ell)}_{1,0}$, $\tilde{\xi}_{3,0}$, $\tilde{\eta}^{(\ell)}_{3,0}$, and p_{1R} only consists of a single-hump profile and the left two-soliton consists of double-hump solitons. The intensity of the double-pole two-soliton consisting of a degenerated single-hump profile remains the same throughout its propagation and it takes a curved path around the interaction regime $z \approx 0$. On the other hand, the other double-pole bright two-soliton can show two types of collision behavior in the bright components u_ℓ ($\ell = 1, 2, \ldots, M-1$): energy-exchanging collision (for $\hat{\tilde{T}}^{(2)}_\ell \neq 1$) and elastic collision (for $\hat{\tilde{T}}^{(2)}_\ell = 1$). However, in the dark component u_M the double-pole dark four-soliton admits elastic collision alone and the degenerated soliton takes a curved path propagation similar to that of the bright soliton.

Case 3. When $\tilde{\xi}_{j,0}$ are finite and $\tilde{\xi}_{s,0} \to \infty$ ($j = 1, 3$ and $s = 2, 4$) or $\tilde{\xi}_{j,0} \to \infty$ and $\tilde{\xi}_{s,0}$ are finite ($j = 1, 3$ and $s = 2, 4$), the bright components u_ℓ and dark component u_M possess completely different dynamical behaviors. In the bright components u_ℓ, one double-pole bright two-soliton completely degenerates into the zero background without any trace. Hence the bright four-soliton behaves similarly to the double-pole two-soliton. However, in the dark component, one dark double-pole two-soliton is transformed into a Peregrine soliton (simplest rogue wave) and the other double-pole dark two-soliton retains its own soliton profile exhibiting elastic interaction. Hence, the dark component u_M supports the coexistence of a dark two-soliton along with a Peregrine soliton. Figure 15 shows such a demonstration resulting for

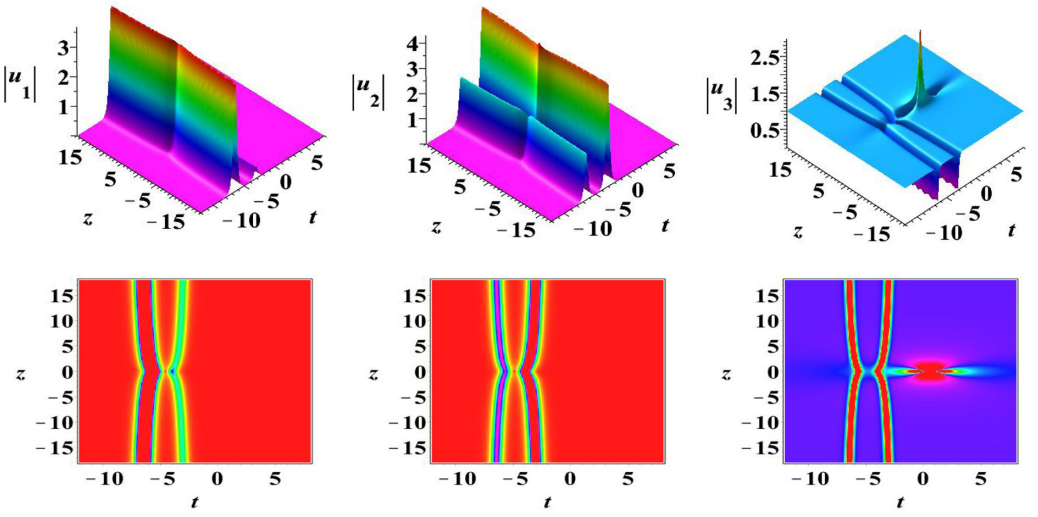

FIG. 15. The top row shows the double-pole bright-dark four-soliton in the focusing 3NLS equation (1) with the parameters $M = 3$, $\delta_1 = 1$, $\delta_2 = 1$, $\delta_3 = 1$, $\tilde{\xi}_{2,0} = -3.2 \times 10^8$, $\tilde{\xi}_{4,0} = 4$, $\tilde{\eta}^{(1)}_{2,0} = 2$, $\tilde{\eta}^{(1)}_{4,0} = 10^8$, $\tilde{\eta}^{(2)}_{2,0} = 1$, $\tilde{\eta}^{(2)}_{4,0} = 10^9$, $p_{1R} = 1$, and $p_{2R} = 4$. The bottom row is the density plot of the top row.

the choice of $\tilde{\xi}_{1,0} \to \infty$ and $\tilde{\xi}_{3,0} \to \infty$ with $\tilde{\xi}_{2,0}$ and $\tilde{\xi}_{4,0}$ chosen to be finite. One can observe the double-pole bright two-soliton in the u_1 and u_2 components and double-pole dark two-soliton coexisting with the Peregrine soliton in the dark component u_3.

The above analysis of the first-order and second-order multicomponent double-pole bright and bright-dark solitons can be straightforwardly extended to an arbitrary Nth-order case with $N \geqslant 3$ too, where several combinations of interaction pictures can be identified along with the collision behaviors discussed in this work. It will be tedious mathematically but will result in interesting outcomes, especially along the direction of rogue wave generation or existence with double-pole dark solitons. Here we have addressed this point with a brief study, but a deeper investigation would be of interest. Further, such rogue wave formation resulting from the double-pole bright solitons is yet another question that needs to be answered through a detailed analysis.

IV. CONCLUSION

In this work we have systematically constructed multicomponent double-pole bright and bright-dark $2N$-solitons of the MCNLS equations (1) comprising all possible combinations of nonlinearities, namely, focusing, defocusing, and mixed nonlinearities arising in different physical settings. This is achieved by taking the long-wavelength limit of the single-pole multicomponent bright-bright and bright-dark soliton pairs through proper parametric choices, which display completely different collision behaviors compared with the standard single-pole solitons. Our analysis of the multicomponent, multiple double-pole bright $2N$-solitons reveals that the focusing and mixed focusing-defocusing MCNLS equations admit the smooth multiple double-pole bright-solitons, while the defocusing MCNLS equations do not have such regular soliton solutions. By analyzing the intensities before and after collision through asymptotic analysis, we have identified two different types of collisions: standard elastic collision and energy-exchanging collision for the first-order double-pole bright (two-soliton with $N = 1$) solitons in the MCNLS equations (1) with $M \geqslant 2$. Additionally, the multiple (second order with $N = 2$ having four-solitons) double-pole two bright $2N$-solitons exhibit the superposition of several individual double-pole two bright two-solitons and possess three types of collisions: elastic collisions, energy-exchanging collisions, and a mixture of elastic collisions and energy-exchanging collisions.

Further in our study we investigated the multiple double-pole bright-dark $2N$-solitons in the MCNLS equations. There exist two types of double-pole bright-dark two-solitons depending on the parameters $\tilde{\xi}_{j,0}$ $(j = 1, 2)$. When $\tilde{\xi}_{1,0}$ and $\tilde{\xi}_{2,0}$ are finite the double-pole bright-dark two-soliton has two soliton waves and a solution exists in the MCNLS equations (1) for all types of nonlinearities, namely, focusing, defocusing, and mixed focusing and defocusing. When $\tilde{\xi}_{1,0} \to \infty$, $\tilde{\xi}_{2,0}$ is finite or $\tilde{\xi}_{1,0}$ is finite and $\tilde{\xi}_{2,0} \to \infty$, the double-pole bright-dark two-solitons only possess a single-soliton wave profile and such a solution exists only for the focusing and mixed (focusing and defocusing) types of MCNLS equations. In the double-pole bright-dark two-soliton, the bright two-solitons can exhibit energy-exchanging collisions when the bright solitons appear in at least two components apart from the elastic collision under different parametric conditions similar to pure bright double-pole solitons, whereas the double-pole dark two-soliton exhibits a mere elastic collision. Further, the multiple (higher-order with $N \geqslant 2$) double-pole bright-dark $2N$-solitons exhibit the superposition of several individual double-pole bright-dark two-solitons, where they possess rich soliton patterns, starting from the degeneration or disappearance of solitons and generation or formation of Peregrine solitons or rogue waves coexisting with double-pole dark soliton pairs. The presented results will be useful to the understanding of multicomponent double-pole bright and bright-dark solitons in the MCNLS equations (1) that appear in different contexts such as nonlinear optics, atomic condensates, and plasma systems and corresponding possible experimental realizations. Further, these outcomes will provide a fundamental platform for investigating various other coupled nonlinear soliton models. An interesting open question about the generation of rogue waves through soliton collisions, which we have addressed here briefly for one case only, can be explored further in detail.

ACKNOWLEDGMENTS

The work of J.R. was supported by Guangdong Basic and Applied Basic Research Foundation (Grant No. 2019A1515110208) and Shenzhen Science and Technology Program (Grant No. RCBS20200714114922203). The work of T.K. was supported by Department of Science and Technology–Science and Engineering Research Board (DST-SERB), Government of India, in the form of a major research project (Project No. EMR/2015/001408). K.S. was supported by DST-SERB National Post-Doctoral Fellowship (Grant No. PDF/2016/000547). The work of J.H. was supported by the National Natural Science Foundation of China (Grants No. 11671219 and No. 12071451).

APPENDIX A: BRIGHT SOLITON SOLUTION OF THE MCNLS EQUATIONS

In this Appendix we present the general bright K-soliton solutions to the MCNLS equations (1), where K is an arbitrary positive integer. The MCNLS equations (1) have the bright K-soliton solutions

$$u_{\ell_{so}} = \frac{g^{(\ell)}(t,z)}{f(t,z)}, \quad \ell = 1, 2, \ldots, M, \tag{A1}$$

where

$$f(t,z) = |M|, \quad g^{(\ell)}(t,z) = \begin{vmatrix} M & \Phi^T \\ -\bar{\Psi}(\ell) & 0 \end{vmatrix}. \tag{A2}$$

The elements of the matrix M are obtained as

$$m_{s,j} = \frac{1}{p_s + p_j^*} e^{\xi_s + \xi_j^*} + \sum_{\ell=1}^{M} \frac{\delta_\ell}{p_s + p_j^*} e^{\eta_{s,0}^{(\ell)} + \eta_{j,0}^{(\ell)*}},$$
$$\xi_s = p_s t + i p_s^2 z + \xi_{s,0}; \; s, j = 1, 2, \ldots, K, \tag{A3}$$

while Φ and $\bar{\Psi}(\ell)$ are row vectors defined by

$$\Phi = (e^{\xi_1}, e^{\xi_2}, \ldots, e^{\xi_K}),$$
$$\bar{\Psi}(\ell) = (e^{\eta_{1,0}^{(\ell)*}}, e^{\eta_{2,0}^{(\ell)*}}, \ldots, e^{\eta_{K,0}^{(\ell)*}}), \quad \ell = 1, 2, \ldots, M. \tag{A4}$$

The superscript T represents the transpose.

We note that the above bright K-soliton solution (A1) and the bright-dark K-soliton solution given in Eq. (B1) are obtained by using the Kadomtsev-Petviashvili hierarchy reduction technique [72–74] combined with Hirota's bilinear method [75]. We only use the $2N$-soliton (i.e., $K = 2N$) solution to derive the double-pole $2N$-soliton solution. The bright and bright-dark K-soliton solutions have also been reported in Refs. [34,37]. Although the determinant forms of the functions f and $g^{(\ell)}$ considered in this work are different, the bright and bright-dark soliton solutions of the present paper can be related to those of Refs. [34,37] by making appropriate transformations to the determinant forms of the functions f and $g^{(\ell)}$. Hence, we refrain from deriving these solutions and will concentrate only on the double-pole solutions and their dynamics in this work.

The double-pole M bright two-soliton is derived by taking the long-wave limit of the bright two-soliton, which is discussed in Sec. II. To realize the conversion from the single-pole two bright two-soliton to the double-pole two bright two-soliton in the MCNLS equations (1) and to identify the complete nature of their collision dynamics, we have discussed the asymptotic behaviors of the bright two-soliton solution with $p_2 = -p_1$. Without loss of generality, we assume $p_{1R} > 0$ and $p_{1I} > 0$, and for convenience we define the right-moving soliton along the line $\tilde{\xi}_1 = t - 2p_{1I}z$ as soliton 1 and the left-moving soliton along the line $\tilde{\xi}_2 = t + 2p_{1I}z$ as soliton 2. The asymptotic expression of the bright two-soliton solution (A1) can be written in the following forms: (a) before collision ($z \to -\infty$), for soliton 1 ($\tilde{\xi}_1 \approx 0$ and $\tilde{\xi}_2 \to -\infty$),

$$u_\ell^{(1)-} \simeq A_\ell^{(1)-} e^{iv_\ell^{(1)}} \operatorname{sech}\left(p_{1R}\tilde{\xi}_1 + \frac{2\xi_{1,0R} + R_1 - R_2}{2}\right), \tag{A5}$$

and for soliton 2 ($\tilde{\xi}_2 \approx 0$ and $\tilde{\xi}_1 \to +\infty$),

$$u_\ell^{(2)-} \simeq A_\ell^{(2)-} e^{iv_\ell^{(2)}} \operatorname{sech}\left(p_{1R}\tilde{\xi}_2 + \frac{\tilde{R}_2 - R_1 - 2\xi_{2,0R}}{2}\right), \tag{A6}$$

and (b) after collision ($z \to +\infty$), for soliton 1 ($\tilde{\xi}_1 \approx 0$ and $\tilde{\xi}_2 \to +\infty$),

$$u_\ell^{(1)+} \simeq A_\ell^{(1)+} e^{i\tilde{v}_\ell^{(1)}} \operatorname{sech}\left(p_{1R}\tilde{\xi}_1 + \frac{2\xi_{1,0R} + \tilde{R}_2 - \tilde{R}_1}{2}\right), \tag{A7}$$

and for soliton 2 ($\tilde{\xi}_2 \approx 0$ and $\tilde{\xi}_1 \to -\infty$),

$$u_\ell^{(2)+} \simeq A_\ell^{(2)+} e^{i\tilde{v}_\ell^{(2)}} \operatorname{sech}\left(p_{1R}\tilde{\xi}_2 + \frac{\tilde{R}_1 - R_2 - 2\xi_{2,0R}}{2}\right). \tag{A8}$$

The auxiliary functions and quantities appearing in the above expressions are defined as

$$A_\ell^{(1)-} = p_{1R}^2\left(\frac{1}{p_{1R}} + \frac{1}{ip_{1I}}\right)e^{\eta_{1,0R}^{(\ell)} - (R_1+R_2)/2},$$
$$v_\ell^{(1)} = \xi_{1,0I} + \tilde{\Phi}_1 - \eta_{1I}^{(\ell)},$$
$$A_\ell^{(2)-} = p_{1R}^2\left(\frac{1}{p_{1R}} + \frac{1}{ip_{1I}}\right)e^{\eta_{2,0R}^{(\ell)} - (R_1+\tilde{R}_2)/2},$$
$$v_\ell^{(1)} = \xi_{2,0I} + \tilde{\Phi}_2 - \eta_{2,0I}^{(\ell)},$$
$$A_\ell^{(1)+} = p_{1R}^2 e^{-(\tilde{R}_1+\tilde{R}_2)/2}\left(-\frac{\tilde{\tilde{m}}_{22}}{p_{1R}}e^{\eta_{1,0}^{(\ell)*}} + \frac{\tilde{\tilde{m}}_{12}^*}{ip_{1I}}e^{\eta_{2,0}^{(\ell)*}}\right),$$
$$\tilde{v}_\ell^{(1)} = \tilde{\Phi}_1 + \xi_{1,0I},$$
$$A_\ell^{(2)+} = p_{1R}^2 e^{-(\tilde{R}_1+R_2)/2}\left(-\frac{\tilde{\tilde{m}}_{12}}{ip_{1I}}e^{\eta_{1,0}^{(\ell)*}} + \frac{\tilde{\tilde{m}}_{11}}{p_{1R}}e^{\eta_{2,0}^{(\ell)*}}\right),$$
$$\tilde{v}_\ell^{(2)} = \tilde{\Phi}_2 + \xi_{2,0I},$$
$$R_1 = \ln\left(1 + \frac{p_{1R}^2}{p_{1I}^2}\right), \quad R_2 = \ln(\tilde{\tilde{m}}_{11}), \quad \tilde{R}_2 = \ln(\tilde{\tilde{m}}_{22}),$$
$$\tilde{\Phi}_1 = p_{1I}t + (p_{1R}^2 - p_{1I}^2)z,$$
$$\tilde{\Phi}_2 = -p_{1I}t + (p_{1R}^2 - p_{1I}^2)t,$$
$$\tilde{R}_1 = \ln\left(\tilde{\tilde{m}}_{11}\tilde{\tilde{m}}_{22} + \frac{p_{1R}^2}{p_{1I}^2}\tilde{\tilde{m}}_{12}\tilde{\tilde{m}}_{12}^*\right), \quad \tilde{\tilde{m}}_{11} = \sum_{k=1}^{M}\delta_k e^{2\eta_{1,0R}^{(k)}},$$
$$\tilde{\tilde{m}}_{22} = \sum_{k=1}^{M}\delta_k e^{2\eta_{2,0R}^{(k)}}, \quad \tilde{\tilde{m}}_{12} = \sum_{k=1}^{M}\delta_k e^{\eta_{1,0}^{(k)} + \eta_{2,0}^{(k)*}}. \tag{A9}$$

From the above asymptotic analysis, we can obtain the details about the following three quantities due to the collision process. (i) The amplitudes of the jth soliton before and after collision in the ℓth component are $|A_\ell^{(j)-}|$ and $|A_\ell^{(j)+}|$, respectively, while the change in these amplitudes is written in terms of the transition relation as

$$|A_\ell^{(j)+}| = T_\ell^{(j)}|A_\ell^{(j)-}|, \quad j = 1, 2; \ \ell = 1, 2, \ldots, M. \tag{A10}$$

In an alternate way the transition amplitude takes the form

$$T_\ell^{(j)} = \frac{|A_\ell^{(j)+}|}{|A_\ell^{(j)-}|}. \tag{A11}$$

(ii) The phase shifts for soliton 1 and soliton 2 are Φ_1 and Φ_2, respectively, which read

$$\Phi_1 = -\Phi_2 = \tfrac{1}{2}(R_2 + \tilde{R}_2 - R_1 - \tilde{R}_1). \tag{A12}$$

(iii) The change in the relative separation distance between the two bright interacting solitons is

$$\Delta t_{12} = \frac{2}{p_{1R}}(R_2 + \tilde{R}_2 - R_1 - \tilde{R}_1) = \frac{2}{p_{1R}}\Phi_1. \tag{A13}$$

In what follows, we consider intensities of the double-pole bright-bright two-soliton solutions given by Eq. (7) before and after collision. Since the double-pole bright-bright two-soliton solutions are translated from the usual (single-pole) bright-bright two-soliton solutions in Eq. (A1) with the parameter conditions given by Eq. (2) through the limiting procedure as $p_{1I} \to 0$, the intensity values of the double-pole bright-bright two solitons can also be converted from the intensity values of the usual (i.e., single-pole) bright-bright two-solitons by the same procedures. Below we calculate the intensity value of soliton 1 before and after collision as an example. To this end, we first insert the parametric condition (2) with $K = 2$ (i.e.,

$N = 1$) into $A_\ell^{(1)-}$; then the expression of $A_\ell^{(1)-}$ is rewritten as

$$A_\ell^{(1)-} = p_{1R}^2\left(\frac{1}{p_{1R}} + \frac{1}{ip_{1I}}\right)p_{1I}\tilde{\eta}_{1,0}^{(\ell)} \times \left[\left(1 + \frac{p_{1R}^2}{p_{1I}^2}\right)\sum_{k=1}^{M}\delta_k\tilde{\eta}_{1,0}^{(k)2}p_{1I}^2\right]^{-1/2}. \quad \text{(A14)}$$

By implementing the limiting producer as $p_{1I} \to 0$ in Eq. (A14), we can obtain the expression of the intensity of the double-pole soliton 1 before collision denoted by $\tilde{A}_\ell^{(1)-}$ in Sec. II in the form

$$\tilde{A}_\ell^{(1)-} = A_\ell^{(1)-}\big|_{p_{1I}\to 0} = -\frac{|p_{1R}|\tilde{\eta}_{1,0}^{(\ell)}i}{\sqrt{\sum_{k=1}^{M}\delta_k\tilde{\eta}_{1,0}^{(k)2}}}. \quad \text{(A15)}$$

Similarly, we can obtain the expression of intensity of the double-pole soliton 2 after collision in the form

$$\tilde{A}_\ell^{(1)+} = -\frac{|p_{1R}|\tilde{\eta}_{2,0}^{(\ell)}}{\sqrt{\sum_{k=1}^{M}\delta_k\tilde{\eta}_{2,0}^{(k)2}}}. \quad \text{(A16)}$$

In this way, the intensity of the double-pole soliton 2 before and after collision can also be as converted from the intensity of the usual (i.e., single-pole) soliton 2, which reads

$$\tilde{A}_\ell^{(2)-} = -\frac{|p_{1R}|\tilde{\eta}_{2,0}^{(\ell)}i}{\sqrt{\sum_{k=1}^{M}\delta_k\tilde{\eta}_{2,0}^{(k)2}}}, \quad \tilde{A}_\ell^{(2)+} = -\frac{|p_{1R}|\tilde{\eta}_{1,0}^{(\ell)}}{\sqrt{\sum_{k=1}^{M}\delta_k\tilde{\eta}_{1,0}^{(k)2}}}. \quad \text{(A17)}$$

APPENDIX B: BRIGHT-DARK SOLITON SOLUTION OF THE MCNLS EQUATIONS

In this Appendix we present the bright-dark K-soliton solution consisting of $M-1$ bright solitons and one dark soliton to the vector MCNLS equations (1). The MCNLS equations (1) have the Kth-order $M-1$ bright, one dark soliton solution

$$u_{\ell_{so}} = e^{2i\delta_M z}\frac{g^{(\ell)}(t,z)}{f(t,z)}, \quad \ell = 1,2,\ldots,M-1, \qquad u_{M_{so}} = e^{2i\delta_M z}\frac{g^{(M)}(t,z)}{f(t,z)}, \quad \text{(B1)}$$

where

$$f = |M^{(0)}|, \quad g^{(\ell)} = \begin{vmatrix} M^{(0)} & \Phi^T \\ -\bar{\Psi}(\ell) & 0 \end{vmatrix}, \quad g^{(M)} = |M^{(1)}|. \quad \text{(B2)}$$

The elements of the matrix $M^{(n)}$ are

$$m_{s,j}^{(n)} = \frac{1}{p_s + p_j^*}\left(-\frac{p_s}{p_j^*}\right)^n e^{\xi_s+\xi_j^*} + \sum_{\ell=1}^{M-1}\frac{\delta_\ell}{\left(p_s + \frac{\delta_M}{p_s}\right) + \left(p_j^* + \frac{\delta_M}{p_j^*}\right)}e^{\eta_{s,0}^{(\ell)}+\eta_{j,0}^{(\ell)*}}, \quad \text{(B3)}$$

$$\xi_s = p_s t + ip_s^2 z + \xi_{s,0};\ s,j = 1,2,\ldots,K,$$

while Φ and $\bar{\Psi}(\ell)$ are row vectors defined by

$$\Phi = (e^{\xi_1}, e^{\xi_2}, \ldots, e^{\xi_K}), \quad \bar{\Psi}(\ell) = (e^{\eta_{1,0}^{(\ell)*}}, e^{\eta_{2,0}^{(\ell)*}}, \ldots, e^{\eta_{K,0}^{(\ell)*}}), \quad \ell = 1,2,\ldots,M-1. \quad \text{(B4)}$$

We note that, throughout our analysis, we have considered the case where all u_ℓ (for $\ell = 1,2,\ldots,M-1$) components admit bright solitons and only the u_M component carries dark solitons.

To understand the single-pole bright-dark two-soliton to double-pole bright-dark two-soliton conversions, first we present the following asymptotic forms of single-pole bright-dark two-soliton [which corresponds to $N = 2$ in Eq. (B2)]: (a) before collision ($z \to -\infty$), for soliton 1 ($\tilde{\xi}_1 \approx 0$ and $\tilde{\xi}_2 \to -\infty$),

$$u_\ell^{(1)-} \simeq \hat{A}_\ell^{(1)-}e^{iv_\ell^{(1)}}\,\mathrm{sech}\left(p_{1R}\tilde{\xi}_1 + \frac{2\xi_{1,0R} + R_1 - \hat{R}_1}{2}\right), \qquad u_M^{(1)-} \simeq \frac{y_1}{2}\left[(y_1+1) + (y_1-1)\tanh\left(p_{1R}\tilde{\xi}_1 + \frac{2\xi_{1,0R} + R_1 - \hat{R}_1}{2}\right)\right], \quad \text{(B5)}$$

and for soliton 2 ($\tilde{\xi}_2 \approx 0$ and $\tilde{\xi}_1 \to +\infty$),

$$u_\ell^{(2)-} \simeq \hat{A}_\ell^{(2)-}e^{iv_\ell^{(2)}}\,\mathrm{sech}\left(p_{1R}\tilde{\xi}_2 + \frac{\hat{R}_2 - R_1 - 2\xi_{2,0R}}{2}\right), \qquad u_M^{(2)-} \simeq \frac{y_1}{2}\left[y_1 + 1 + (y_1-1)\tanh\left(p_{1R}\tilde{\xi}_2 + \frac{\hat{R}_2 - R_1 - 2\xi_{2,0R}}{2}\right)\right], \quad \text{(B6)}$$

and (b) after collision ($z \to +\infty$), for soliton 1 ($\tilde{\xi}_1 \approx 0$ and $\tilde{\xi}_2 \to +\infty$),

$$u_\ell^{(1)+} \simeq \hat{A}_\ell^{(1)+}e^{i\tilde{v}_\ell^{(1)}}\,\mathrm{sech}\left(p_{1R}\tilde{\xi}_1 + \frac{2\xi_{1,0R} + \hat{R}_2 - \hat{R}_0}{2}\right), \qquad u_M^{(1)+} \simeq \frac{1}{2}\left[y_1 + 1 + (y_1-1)\tanh\left(p_{1R}\tilde{\xi}_1 + \frac{2\xi_{1,0R} + \hat{R}_2 - \hat{R}_0}{2}\right)\right], \quad \text{(B7)}$$

and for soliton 2 ($\tilde{\xi}_2 \approx 0$ and $\tilde{\xi}_1 \to -\infty$),

$$u_\ell^{(2)+} \simeq \hat{A}_\ell^{(2)+} e^{i\tilde{v}_\ell^{(2)}} \operatorname{sech}\left(p_{1R}\tilde{\xi}_2 + \frac{\hat{R}_0 - \hat{R}_1 - 2\xi_{2,0R}}{2}\right),$$
$$u_M^{(2)+} \simeq \frac{1}{2}\left[y_1 + 1 + (y_1 - 1)\tanh\left(p_{1R}\tilde{\xi}_2 + \frac{\hat{R}_0 - \hat{R}_1 - 2\xi_{2,0R}}{2}\right)\right]. \tag{B8}$$

The auxiliary functions and the various quantities in these expressions are defined by

$$\hat{A}_\ell^{(1)-} = p_{1R}^2\left(\frac{1}{p_{1R}} + \frac{1}{ip_{1I}}\right)e^{\eta_{1,0R}^{(\ell)} - (\hat{R}_1 + R_1)/2}, \quad v_\ell^{(1)} = \xi_{1,0I} + \tilde{\Phi}_1 - \eta_{1I}^{(\ell)},$$
$$\hat{A}_\ell^{(2)-} = p_{1R}^2\left(\frac{1}{p_{1R}} + \frac{1}{ip_{1I}}\right)e^{\eta_{2,0R}^{(\ell)} - (\hat{R}_2 + R_1)/2}, \quad v_\ell^{(1)} = \xi_{2,0I} + \tilde{\Phi}_2 - \eta_{2,0I}^{(\ell)},$$
$$\hat{A}_\ell^{(1)+} = p_{1R}^2 e^{-(\hat{R}_2 + \hat{R}_0)/2}\left(-\frac{\hat{\tilde{m}}_{22}}{q_{1R}}e^{\eta_{1,0}^{(\ell)*}} + \frac{\hat{\tilde{m}}_{12}^*}{iq_{1I}}e^{\eta_{2,0}^{(\ell)*}}\right), \quad \tilde{v}_\ell^{(1)} = \tilde{\Phi}_1 + \xi_{1,0I},$$
$$\hat{A}_\ell^{(2)+} = p_{1R}^2 e^{-(\hat{R}_0 + \hat{R}_1)/2}\left(-\frac{\hat{\tilde{m}}_{12}}{iq_{1I}}e^{\eta_{1,0}^{(\ell)*}} + \frac{\hat{\tilde{m}}_{11}}{q_{1R}}e^{\eta_{2,0}^{(\ell)*}}\right), \quad \tilde{v}_\ell^{(2)} = \tilde{\Phi}_2 + \xi_{2,0I},$$
$$\hat{R}_1 = \ln\left(\frac{p_{1R}}{q_{1R}}\hat{\tilde{m}}_{11}\right), \quad \hat{R}_2 = \ln\left(\frac{p_{1R}}{q_{1R}}\hat{\tilde{m}}_{22}\right), \tag{B9}$$
$$\tilde{\Phi}_1 = p_{1I}t + \left(p_{1R}^2 - p_{1I}^2\right)z, \quad \tilde{\Phi}_2 = -p_{1I}t + \left(p_{1R}^2 - p_{1I}^2\right)t,$$
$$\hat{R}_0 = \ln\left(\frac{p_{1R}^2}{q_{1R}^2}\hat{\tilde{m}}_{11}\hat{\tilde{m}}_{22} + \frac{p_{1R}^2}{q_{1I}^2}\hat{\tilde{m}}_{12}\hat{\tilde{m}}_{12}^*\right), \quad \hat{\tilde{m}}_{11} = \sum_{k=1}^{M-1}\delta_k e^{2\eta_{1,0R}^{(k)}},$$
$$\hat{\tilde{m}}_{22} = \sum_{k=1}^{M-1}\delta_k e^{2\eta_{2,0R}^{(k)}}, \quad \hat{\tilde{m}}_{12} = \sum_{k=1}^{M-1}\delta_k e^{\eta_{1,0}^{(k)} + \eta_{2,0}^{(k)*}},$$
$$y_1 = -\frac{p_1}{p_1^*}, \quad q_1 = p_1 + \frac{\delta_M}{p_1}.$$

From the above asymptotic analysis, we can obtain that for the component u_ℓ ($\ell = 1, 2, \ldots, M-1$), corresponding to bright solitons, the amplitudes of the jth soliton before and after collision are $|\hat{A}_\ell^{(j)-}|$ and $|\hat{A}_\ell^{(j)+}|$, respectively, and the transition amplitudes of jth soliton are

$$\left|\hat{A}_\ell^{(j)+}\right| = \hat{T}_\ell^{(j)}\left|\hat{A}_\ell^{(j)-}\right|, \quad \left|\hat{A}_M^{(j)+}\right| = \left|\frac{1}{y_1}\right|\left|\hat{A}_M^{(j)-}\right|, \tag{B10}$$

namely,

$$\hat{T}_\ell^{(j)} = \frac{\left|\hat{A}_\ell^{(j)+}\right|}{\left|\hat{A}_\ell^{(j)-}\right|}, \quad \hat{T}_M^{(j)} = \left|\frac{1}{y_1}\right|, \tag{B11}$$

where $j = 1, 2$ and $\ell = 1, 2, \ldots, M-1$. For the u_M component, corresponding to dark solitons, the amplitudes of the jth dark soliton before and after collision are

$$\left|\hat{A}_M^{(j)-}\right| = \tfrac{1}{2}|y_1(y_1+1)|, \quad \left|\hat{A}_M^{(j)+}\right| = \tfrac{1}{2}|y_1+1| \tag{B12}$$

and the transition amplitude of the jth dark soliton is

$$\hat{T}_M^{(j)} = \left|\frac{1}{y_1}\right|. \tag{B13}$$

Since $|y_1| = 1$, i.e., $T_M = 1$, the dark two-soliton undergoes elastic collision in the u_M component. Additionally, the phase shifts for the two-soliton solution are given by the expression

$$\hat{\Phi}_1 = -\hat{\Phi}_2 = \tfrac{1}{2}(\hat{R}_2 + \hat{R}_1 - \hat{R}_0 - R_1), \tag{B14}$$

where $\hat{\Phi}_j$ denotes the phase shift for the jth soliton. The exact form of the changes in relative distance between the two-soliton reads

$$\hat{\Delta}t_{12} = \frac{2}{p_{1R}}(\hat{R}_2 + \hat{R}_1 - \hat{R}_0 - \hat{R}_1) = \frac{2}{p_{1R}}\Phi_1. \tag{B15}$$

[1] Y. S. Kivshar and G. P. Agrawal, *Optical Solitons: From Fibers to Photonic Crystals* (Academic, San Diego, 2003).

[2] M. Ablowitz, B. Prinari, and A. Trubatch, *Discrete and Continuous Nonlinear Schrödinger Systems* (Cambridge University Press, Cambridge, 2003).

[3] P. G. Kevrekidis and D. J. Frantzeskakis, Solitons in coupled nonlinear Schrödinger models: A survey of recent developments, Rev. Phys. **1**, 140 (2016).

[4] A. C. Scott, *Nonlinear Science: Emergence and Dynamics of Coherent Structures* (Oxford University Press, Oxford, 1999).

[5] C. Pethick and H. Smith, *Bose-Einstein Condensation in Dilute Gases* (Cambridge University Press, Cambridge, 2002); P. G. Kevrekidis, D. J. Frantzeskakis, and R. Carretero-Gonzàlez, *Emergent Nonlinear Phenomena in Bose-Einstein Condensates: Theory and Experiment* (Springer, Heidelberg, 2008); M. Ueda, *Fundamentals and New Frontiers of Bose-Einstein Condensation* (World Scientific, Singapore, 2010).

[6] C. Menyuk, Pulse propagation in an elliptically birefringent Kerr media, IEEE J. Quantum Electron. **25**, 2674 (1989).

[7] B. J. Eggleton, R. E. Slusher, C. M. de Sterke, P. A. Krug, and J. E. Sipe, Bragg Grating Solitons, Phys. Rev. Lett. **76**, 1627 (1996); D. Rand, K. Steiglitz, and P. R. Prucnal, Multicomponent gap solitons in superposed grating structures, Opt. Lett. **30**, 1695 (2005).

[8] N. Lazarides and G. P. Tsironis, Coupled nonlinear Schrödinger field equations for electromagnetic wave propagation in nonlinear left-handed materials, Phys. Rev. E **71**, 036614 (2005).

[9] D. J. Kaup, A. Reiman, and A. Bers, Space-time evolution of nonlinear three-wave interactions in a homogeneous medium, Rev. Mod. Phys. **51**, 275 (1979); A. Degasperis, M. Conforti, F. Baronio, and S. Wabnitz, Stable Control of Pulse Speed in Parametric Three-Wave Solitons, Phys. Rev. Lett. **97**, 093901 (2006).

[10] D. N. Christodoulides, T. H. Coskun, M. Mitchell, and M. Segev, Theory of Incoherent Self-Focusing in Biased Photorefractive Media, Phys. Rev. Lett. **78**, 646 (1997).

[11] V. E. Zakharov and E. I. Schulman, To the integrability of the system of two coupled nonlinear Schrödinger equations, Physica D **4**, 270 (1982); V. G. Makhankov and O. K. Pashaev, Nonlinear Schrödinger equation with noncompact isogroup, Theor. Math. Phys. **53**, 979 (1982); A. P. Fordy and P. P. Kulish, Nonlinear Schrödinger equations and simple Lie algebras, Commun. Math. Phys. **89**, 427 (1983); R. Radhakrishnan, R. Sahadevan, and M. Lakshmanan, Integrability and singularity structure of coupled nonlinear Schrödinger equations, Chaos Soliton. Fractal. **5**, 2315 (1995).

[12] S. V. Manakov, On the theory of two-dimensional stationary self-focusing of electromagnetic waves, Zh. Eksp. Teor. Fiz. **65**, 505 (1973) [Sov. Phys. JETP **38**, 248 (1974)].

[13] R. Radhakrishnan, M. Lakshmanan, and J. Hietarinta, Inelastic collision and switching of coupled bright solitons in optical fibers, Phys. Rev. E **56**, 2213 (1997).

[14] N. Akhmediev, A. Ankiewicz, and J. M. Soto-Crespo, Rogue waves and rational solutions of the nonlinear Schrödinger equation, Phys. Rev. E **80**, 026601 (2009).

[15] T. Kanna and M. Lakshmanan, Exact Soliton Solutions, Shape Changing Collisions, and Partially Coherent Solitons in Coupled Nonlinear Schrödinger Equations, Phys. Rev. Lett. **86**, 5043 (2001).

[16] A. Degasperis, M. Conforti, F. Baronio, and S. Wabnitz, Effects of nonlinear wave coupling: Accelerated solitons, Eur. Phys. J. Spec. Top. **147**, 233 (2007).

[17] S. Chen, J. M. Soto-Crespo, and P. Grelu, Dark three-sister rogue waves in normally dispersive optical fibers with random birefringence, Opt. Express **22**, 27632 (2014).

[18] J. Rao, K. Porsezian, T. Kanna, Y. Cheng, and J. He, Vector rogue waves in integrable M-coupled nonlinear Schrödinger equations, Phys. Scr. **94**, 075205 (2019).

[19] K. Krupa, A. Tonello, A. Barthélémy, T. Mansuryan, V. Couderc, G. Millot, P. Grelu, D. Modotto, S. A. Babin, and S. Wabnitz, Multimode nonlinear fiber optics, a spatiotemporal avenue, APL Photon. **4**, 110901 (2019).

[20] J. Rao, K. Porsezian, J. He, and T. Kanna, Dynamics of lumps and dark–dark solitons in the multi-component long-wave–short-wave resonance interaction system, Proc. R. Soc. A **474**, 20170627 (2018).

[21] A. S. Desyatnikov and Y. S. Kivshar, Necklace-Ring Vector Solitons, Phys. Rev. Lett. **87**, 033901 (2001).

[22] K. Sakkaravarthi, T. Kanna, M. Vijayajayanthi, and M. Lakshmanan, Multicomponent long-wave–short-wave resonance interaction system: Bright solitons, energy-sharing collisions, and resonant solitons, Phys. Rev. E **90**, 052912 (2014).

[23] D. Mihalache, Multidimensional localized structures in optical and matter-wave media: A topical survey of recent literature, Romanian Rep. Phys. **69**, 403 (2017).

[24] S. Chakravarty, M. J. Ablowitz, J. R. Sauer, and R. B. Jenkins, Multisoliton interactions and wavelength-division multiplexing, Opt. Lett. **20**, 136 (1995).

[25] C. Yeh and L. Bergman, Enhanced pulse compression in a nonlinear fiber by a wavelength division multiplexed optical pulse, Phys. Rev. E **57**, 2398 (1998).

[26] F. Poletti and P. Horak, Description of ultrashort pulse propagation in multimode optical fibers, J. Opt. Soc. Am. B **25**, 1645 (2008); A. Mecozzi, C. Antonelli, and M. Shtaif, Nonlinear propagation in multi-mode fibers in the strong coupling regime, Opt. Exp. **20**, 11673 (2012); S. Mumtaz, R. J. Essiambre, and G. P. Agrawal, Nonlinear propagation in multimode and multicore fibers: Generalization of the Manakov equations, J. Lightw. Technol. **31**, 398 (2013).

[27] C. Anastassiou, M. Segev, K. Steiglitz, J. A. Giordmaine, M. Mitchell, M.-F. Shih, S. Lan, and J. Martin, Energy-Exchange Interactions between Colliding Vector Solitons, Phys. Rev. Lett. **83**, 2332 (1999).

[28] A. P. Sheppard and Y. S. Kivshar, Polarized dark solitons in isotropic Kerr media, Phys. Rev. E **55**, 4773 (1997).

[29] R. Radhakrishnan and M. Lakshmanan, Bright and dark soliton solutions to coupled nonlinear Schrödinger equations, J. Phys. A: Math. Gen. **28**, 2683 (1995).

[30] M. Vijayajayanthi, T. Kanna, and M. Lakshmanan, Bright-dark solitons and their collisions in mixed N-coupled nonlinear Schrödinger equations, Phys. Rev. A **77**, 013820 (2008).

[31] T. Kanna, M. Lakshmanan, P. Tchofo Dinda, and N. Akhmediev, Soliton collisions with shape change by intensity redistribution in mixed coupled nonlinear Schrödinger equations, Phys. Rev. E **73**, 026604 (2006).

[32] Y. V. Bludov, V. V. Konotop, and N. Akhmediev, Vector rogue waves in binary mixtures of Bose-Einstein condensates, Eur. Phys. J. Spec. Top. **185**, 169 (2010); G. Mu, Z. Qin, and R. Grimshaw, Dynamics of rogue waves on a multisoliton background in a vector nonlinear Schrödinger equation, SIAM J. Appl. Math. **75**, 1 (2015).

[33] T. Kanna and M. Lakshmanan, Exact soliton solutions of coupled nonlinear Schrödinger equations: Shape-changing collisions, logic gates, and partially coherent solitons, Phys. Rev. E **67**, 046617 (2003).

[34] M. Vijayajayanthi, T. Kanna, and M. Lakshmanan, Multisoliton solutions and energy sharing collisions in coupled nonlinear Schrödinger equations with focusing, defocusing and mixed type nonlinearities, Eur. Phys. J. Spec. Top. **173**, 57 (2009).

[35] T. Kanna, K. Sakkaravarthi, and M. Vijayajayanthi, Novel energy sharing collisions of multicomponent solitons, Pramana-J. Phys. **85**, 881 (2015).

[36] Q.-H. Park and H. J. Shin, Systematic construction of multicomponent optical solitons, Phys. Rev. E **61**, 3093 (2000).

[37] B. Feng, General N-soliton solution to a vector nonlinear Schrödinger equation, J. Phys. A: Math. Theor. **47**, 355203 (2014).

[38] Y. Ohta, D.-S. Wang, and J. Yang, General N-dark–dark solitons in the coupled nonlinear Schrödinger equations, Stud. Appl. Math. **127**, 345 (2011).

[39] L. Ling, L. Zhao, and B. Guo, Darboux transformation and multi-dark soliton for N-component nonlinear Schrödinger equations, Nonlinearity **28**, 3243 (2015).

[40] B. Prinari, M. J. Ablowitz, and G. Biondini, Inverse scattering transform for the vector nonlinear Schrödinger equation with nonvanishing boundary conditions, J. Math. Phys. **47**, 063508 (2006).

[41] G. Zhang and Y. Yan, The n-component nonlinear Schrödinger equations: Dark–bright mixed N- and high-order solitons and breathers, and dynamics, Proc. R. Soc. A **474**, 20170688 (2018).

[42] V. Zakharov and A. Shabat, Exact theory of two-dimensional self–focusing and one-dimensional self-modulation of waves in nonlinear media, Sov. Phys. JETP **34**, 62 (1972).

[43] L. Gagon and N. Stiévenart, N-soliton interaction in optical fibers: The multiple-pole case, Opt. Lett. **19**, 619 (1994).

[44] T. Aktosun, F. Demontis, and C. van der Mee, Exact solutions to the focusing nonlinear Schrödinger equation, Inverse Probl. **23**, 2171 (2007).

[45] T. N. B. Martines, Generalized inverse scattering transform for the nonlinear Schrödinger equation for bound states with higher multiplicities, Electron. J. Differ. Equ. **179**, 1 (2017).

[46] S. Tanaka, Non-linear Schrödinger equation and modified Korteweg–de Vries equation; construction of solutions in terms of scattering data, Publ. Res. Inst. Math. Sci. Kyoto **10**, 329 (1975).

[47] E. Olmedilla, Multiple pole solutions of the non-linear Schrödinger equation, Physica D **25**, 330 (1987).

[48] C. Schiebold, Asymptotics for the multiple pole solutions of the nonlinear Schrödinger equation, Nonlinearity **30**, 2930 (2017).

[49] D. Bilman and R. Buckingham, Large-order asymptotics for multiple-pole solitons of the focusing nonlinear Schrödinger equation, J. Nonlinear Sci. **29**, 2185 (2019).

[50] M. Wadati and K. Ohkuma, Multiple-pole solutions of the modified Korteweg–de Vries equation, J. Phys. Soc. Jpn. **51**, 2029 (1982).

[51] D. J. Zhang, S. L. Zhao, Y. Y. Sun, and J. Zhou, Solutions to the modified Korteweg–de Vries equation, Rev. Math. Phys. **26**, 1430006 (2014).

[52] T. Aktosun, F. Demontis, and C. van der Mee, Exact solutions to the sine-Gordon equation, J. Math. Phys. **51**, 123521 (2010).

[53] C. Pöppe, Construction of solutions of the sine-Gordon equation by means of Fredholm determinants, Physica D **9**, 103 (1983).

[54] H. Tsuru and M. Wadati, The multiple pole solutions of the sine-Gordon equation, J. Phys. Soc. Jpn. **53**, 2908 (1984).

[55] V. Shchesnovich and J. Yang, Higher-order solitons in the N-wave system, Stud. Appl. Math. **110**, 297 (2003).

[56] Y. Kuang and J. Zhu, The higher-order soliton solutions for the coupled Sasa-Satsuma system via the ∂-dressing method, Appl. Math. Lett. **66**, 47 (2017).

[57] D. W. C. Lai, K. W. Chow, and K. Nakkeeran, Multiple-pole soliton interactions in optical fibres with higher-order effects, J. Mod. Opt. **51**, 455 (2004).

[58] M. Li, X. Zhang, T. Xu, and L. Li, Asymptotic analysis and soliton interactions of the multi-pole solutions in the Hirota equation, J. Phys. Soc. Jpn. **89**, 054004 (2020).

[59] X. Zhang and L. Ling, Asymptotic analysis of high order solitons for the Hirota equation, arXiv:2008.12631.

[60] D. Bian, B. Guo, and L. Ling, High-order soliton solution of Landau-Lifshitz equation, Stud. Appl. Math. **134**, 181 (2015).

[61] Y. Zhang, J. Rao, J. He, and Y. Cheng, Riemann-Hilbert method for the Wadati-Konno-Ichikawa equation: Simple poles and one higher-order pole, Physica D **399**, 173 (2019).

[62] M. Li, X. Yue, and T. Xu, Multi-pole solutions and their asymptotic analysis of the focusing Ablowitz-Ladik equation, Phys. Scr. **95**, 055222 (2020).

[63] D. W. C. Lai and K. W. Chow, 'Positon' and 'dromion' solutions of the $(2+1)$ dimensional long wave-short wave resonance interaction equations, J. Phys. Soc. Jpn. **68**, 1847 (1999).

[64] K. W. Chow, D. W. C. Lai, C. K. Shek, and K. Tso, Positon-like solutions of nonlinear evolution equations in $(2+1)$ dimensions, Chaos Soliton. Fractal. **9**, 1901 (1998).

[65] V. Matveev, Generalized Wronskian formula for solutions of the KdV equations: First applications, Phys. Lett. A **166**, 205 (1992).

[66] V. Matveev, Asymptotics of the multi-positon-soliton τ function of the Korteweg–de Vries equation and the supertransparency, J. Math. Phys. **35**, 2955 (1994).

[67] R. Beutler, Positon solutions of the sine-Gordon equation, J. Math. Phys. **34**, 3098 (1993).

[68] M. Jaworski and J. Zagrodzinski, Positon and positon-like solutions of the Korteweg–de Vries and sine-Gordon equations, Chaos Soliton. Fractal. **5**, 2229 (1995).

[69] C. Rasinariu, U. Sukhatme, and A. Khare, Negaton and positon solutions of the KdV and mKdV hierarchy, J. Phys. A: Math. Gen. **29**, 1803 (1996).

[70] K. W. Chow and D. W. C. Lai, Coalescence of wavenumbers and exact solutions for a system of couple nonlinear Schrödinger equations, J. Phys. Soc. Jpn. **67**, 3721 (1998).

[71] G. Biondini and D. Kraus, Inverse scattering transform for the defocusing Manakov system with nonzero boundary conditions, SIAM J. Math. Anal. **47**, 706 (2015).

[72] M. Sato, Soliton equations as dynamical systems on an infinite dimensional Grassmann manifold, Res. Inst. Math. Sci. Kokyuroku **439**, 30 (1981).

[73] M. Jimbo and T. Miwa, Solitons and infinite dimensional Lie algebras, Res. Inst. Math. Sci. Kyoto **19**, 943 (1983).

[74] E. Date, M. Kashiwara, M. Jimbo, and T. Miwa, in *Proceedings of RIMS Symposium on Nonlinear Integrable Systems—Classical Theory and Quantum Theory, Kyoto, 1981*, edited by M. Jimbo and T. Miwa (World Scientific, Singapore, 1983), pp. 39–119.

[75] R. Hirota, *The Direct Method in Soliton Theory* (Cambridge University Press, Cambridge, 2004).